SAND2022-11442C

A hybrid mesh-based/element-free method using fine-scale triangulations for the solution of PDEs on geometrically complex domains without defeaturing

Joe Bishop

Engineering Sciences Center
Sandia National Laboratories
Albuquerque, NM

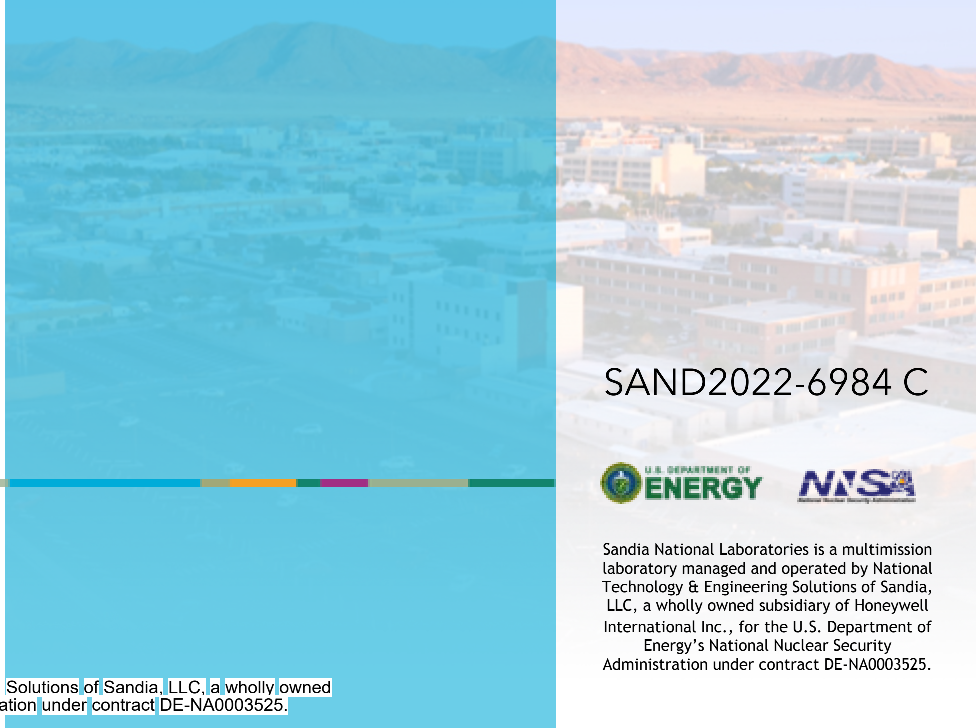

SAND2022-6984 C

ASME IMECE, October 30 – November 3, 2022, Columbus, OH

Sandia National Laboratories is a multimission laboratory managed and operated by National Technology & Engineering Solutions of Sandia, LLC, a wholly owned subsidiary of Honeywell International Inc., for the U.S. Department of Energy's National Nuclear Security Administration under contract DE-NA0003525.

Outline

1. motivation
2. hybrid mesh/element-free discretizations
3. weight functions using manifold geodesics
4. shape functions using moving least squares
5. quadrature via secondary basis functions
6. strain projections for polynomial consistency
7. verification example, linear elasticity
8. summary

Motivation: Image-based analysis

Johnson, et al., 2019, “Predicting the reliability of an additively-manufactured metal part for the third Sandia fracture challenge by accounting for random material defects,” *International Journal of Fracture*, v. 218, pp. 231-243

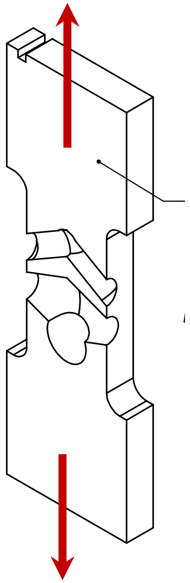

cut-away view

strain field

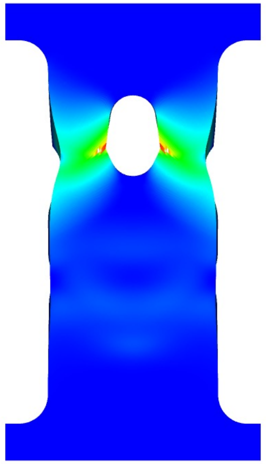

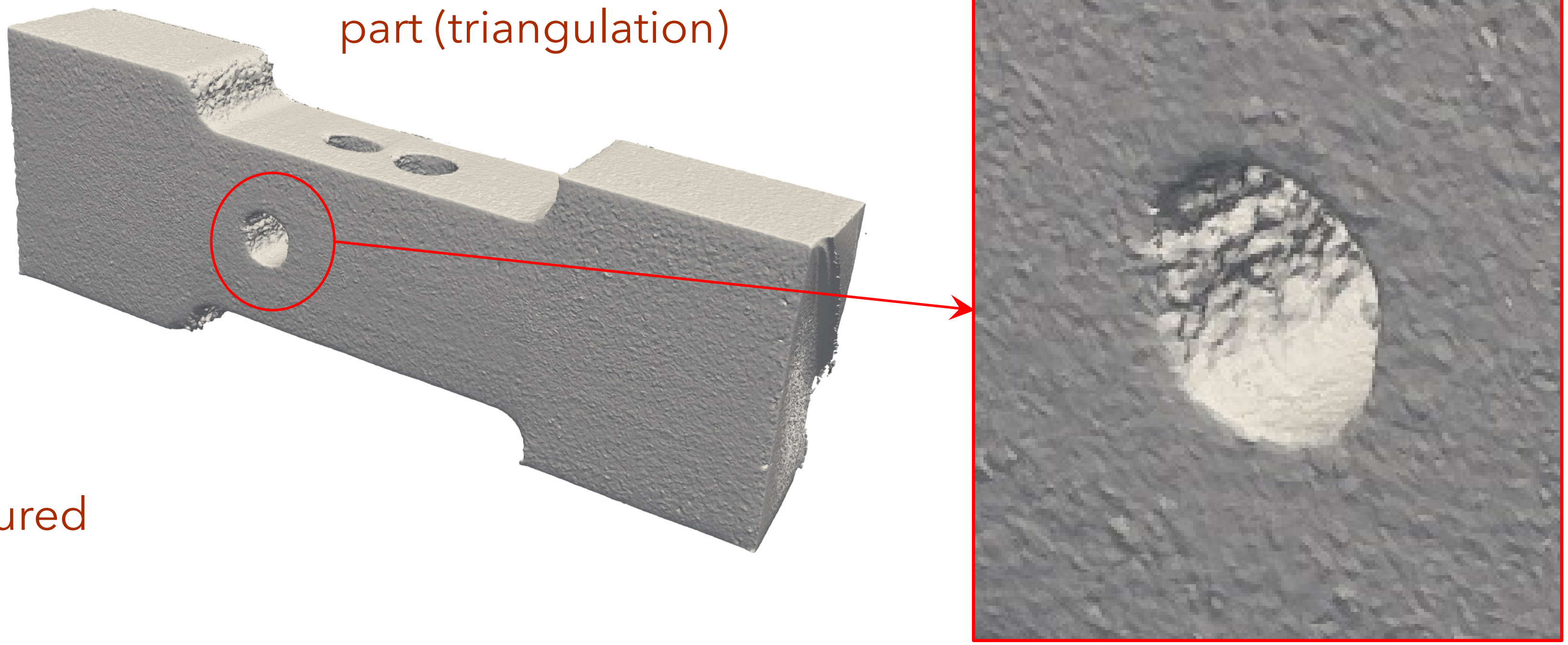

CT reconstruction of AM part (triangulation)

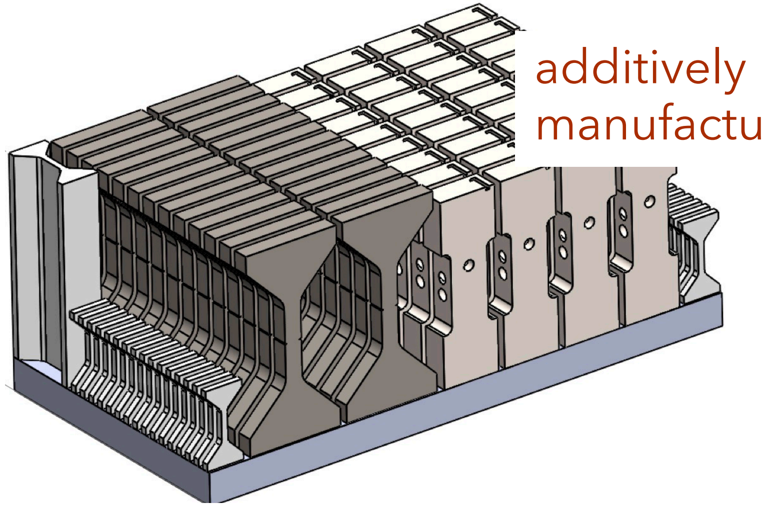

additively manufactured

Typical geometric reconstructions require a smoothing or decimation process before modeling can commence.

Motivation: Agile simulation of complex assemblies

hermetic electrical connector

chamfer

fillet

thread

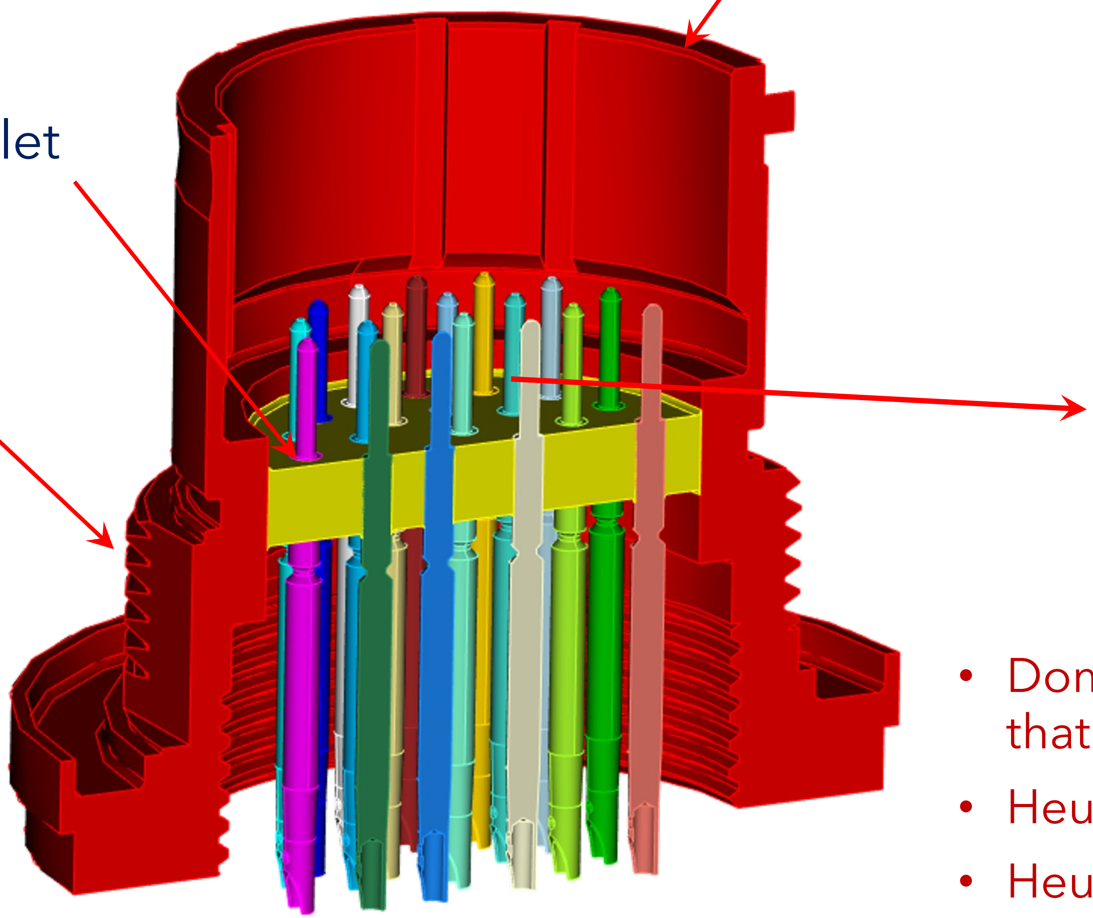

stress field in glass seal after manufacturing

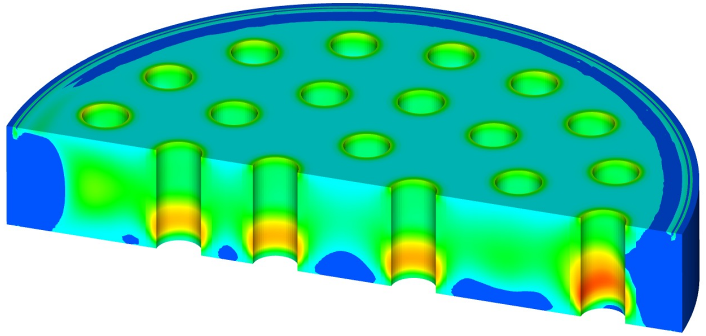

- Domains typically contain many geometric features that must be removed before analysis.
- Heuristics are often used to defeature geometry.
- Heuristics are used to construct finite element mesh.

Motivation: Agile simulation

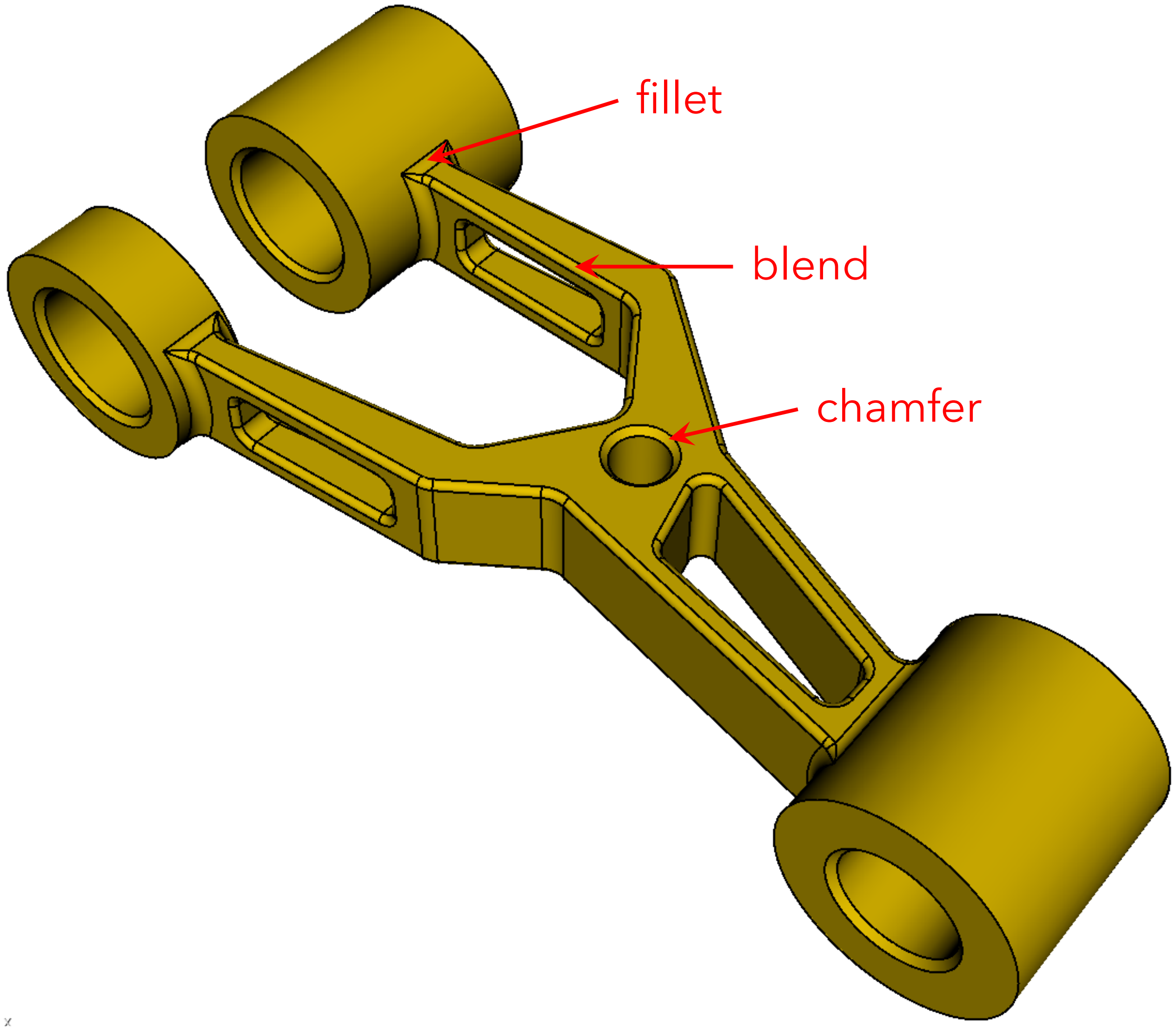

Motivation: Agile simulation

FEA discretization is intimately tied to domain geometry.

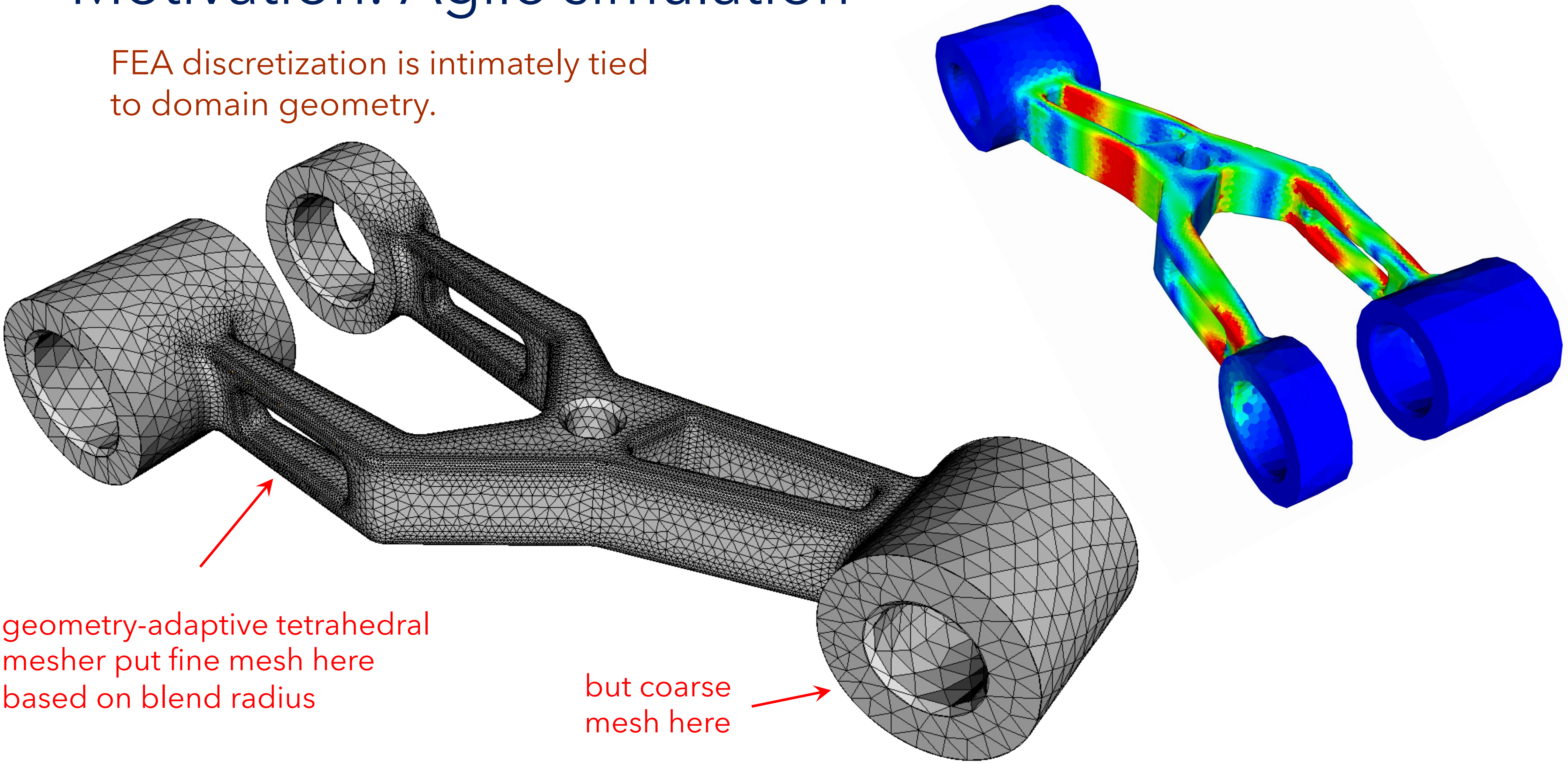

geometry-adaptive tetrahedral mesher put fine mesh here based on blend radius

but coarse mesh here

Motivation: Separate domain discretization from solution discretization

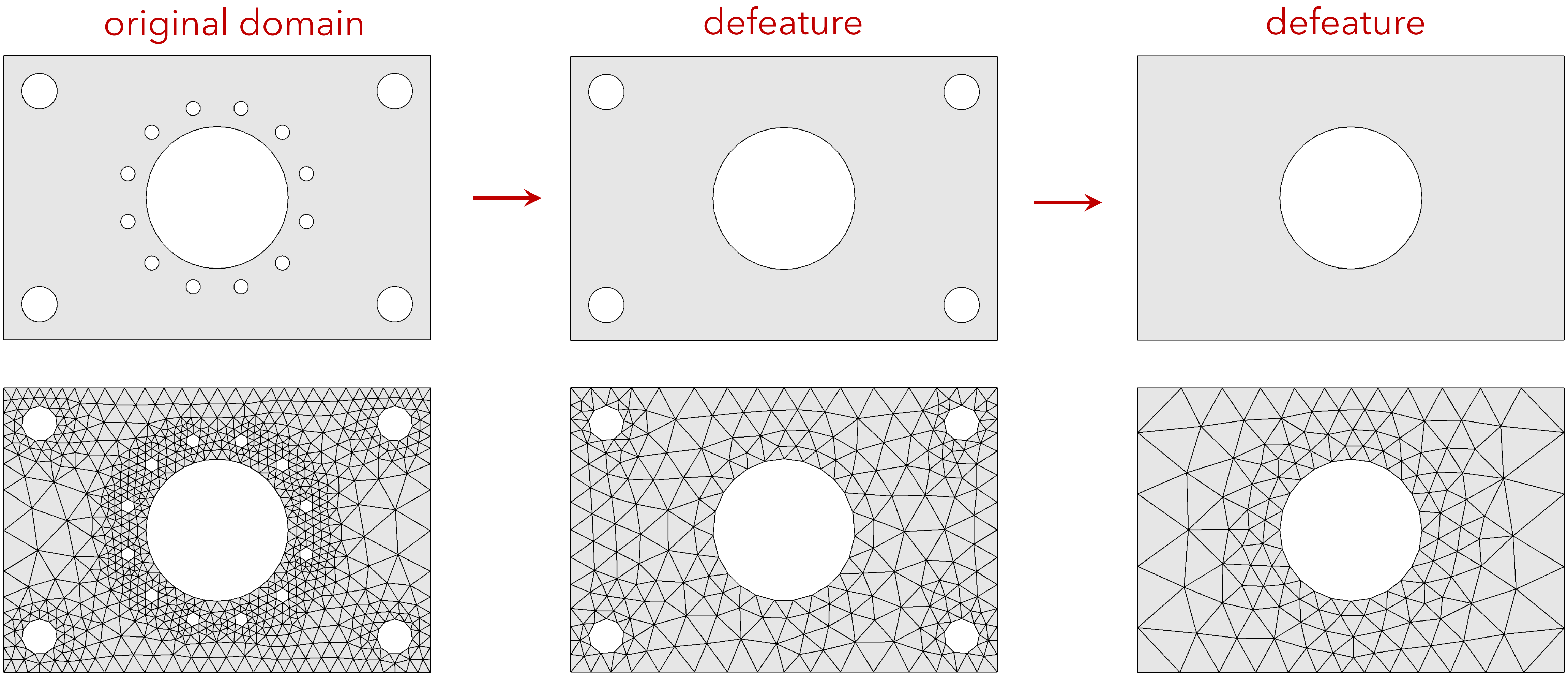

Impact of domain defeaturing? depends on goals of simulation

Hybrid approach: fine-scale triangulation

original domain

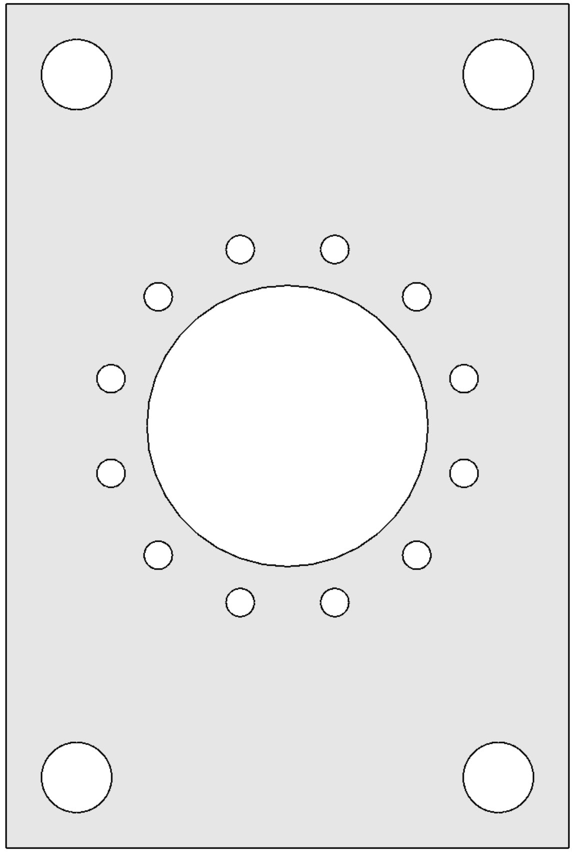

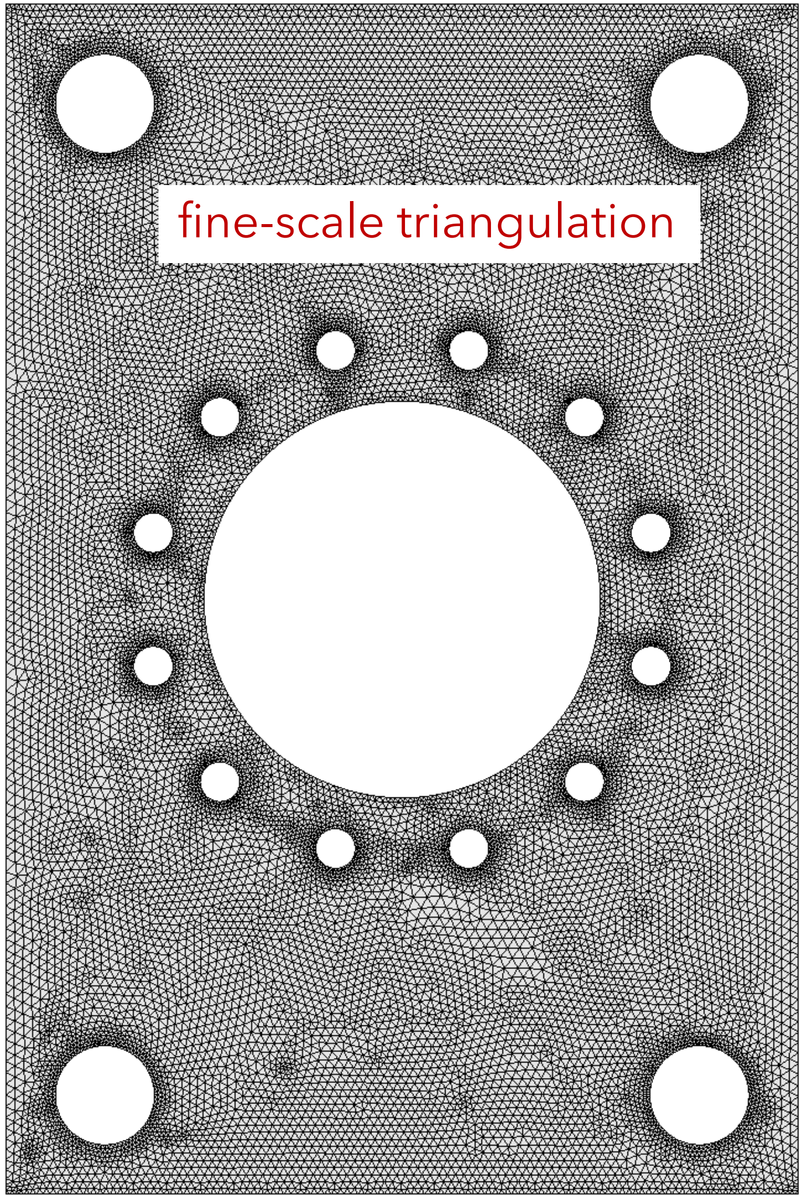

fine-scale triangulation

create an element-free
basis using triangulation.

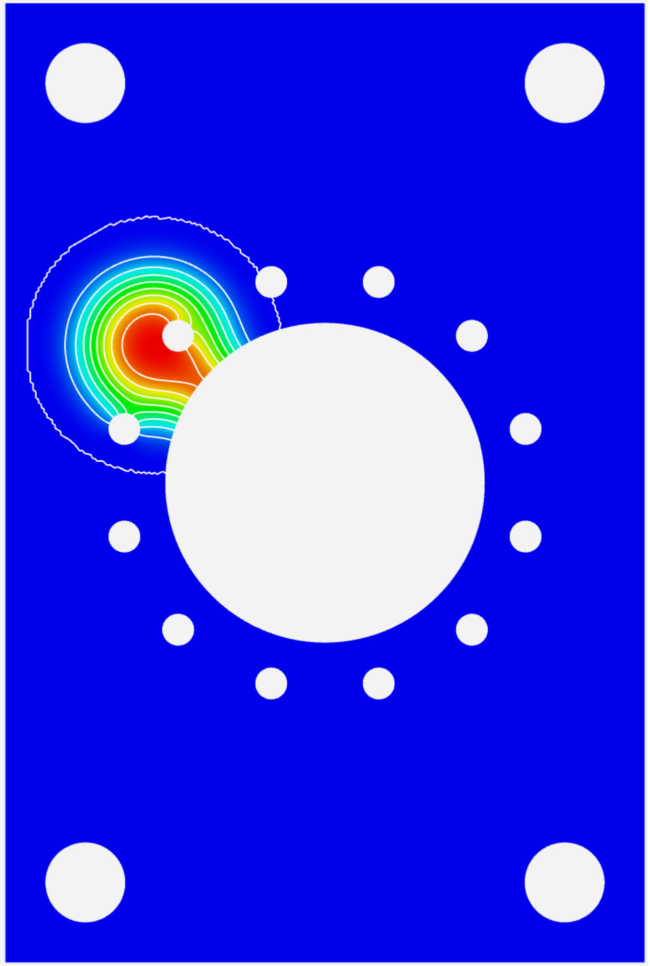

Element-free basis functions

- Element-free basis functions automatically include geometric features at all scales.
- Solution discretization is separate from domain discretization.
- No need to defeature domain.
- PDE solution is insensitive to quality of fine-scale triangulation.

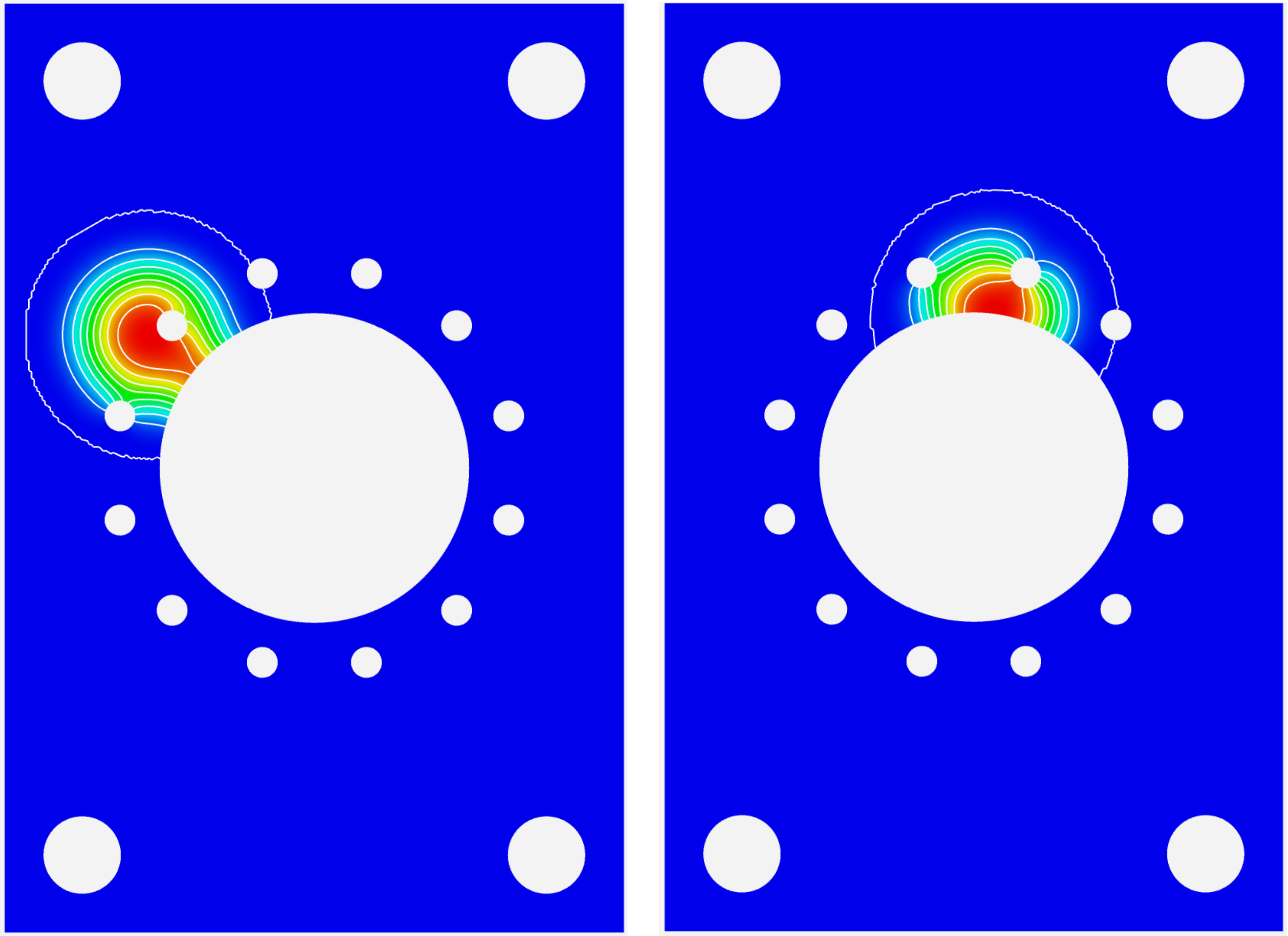

Hybrid approach: fine-scale triangulation

Tet-meshing methods

- Delaunay
- advancing front
- background grid
- envelope

TetWild

Fast Tetrahedral Meshing in the Wild

ACM Trans. Graph. 2020
vol. 39 Issue 4 Article 117

YIXIN HU, New York University, USA
TESEO SCHNEIDER, New York University, USA
BOLUN WANG, Beihang University, China and New York University, USA
DENIS ZORIN, New York University, USA
DANIELE PANOZZO, New York University, USA

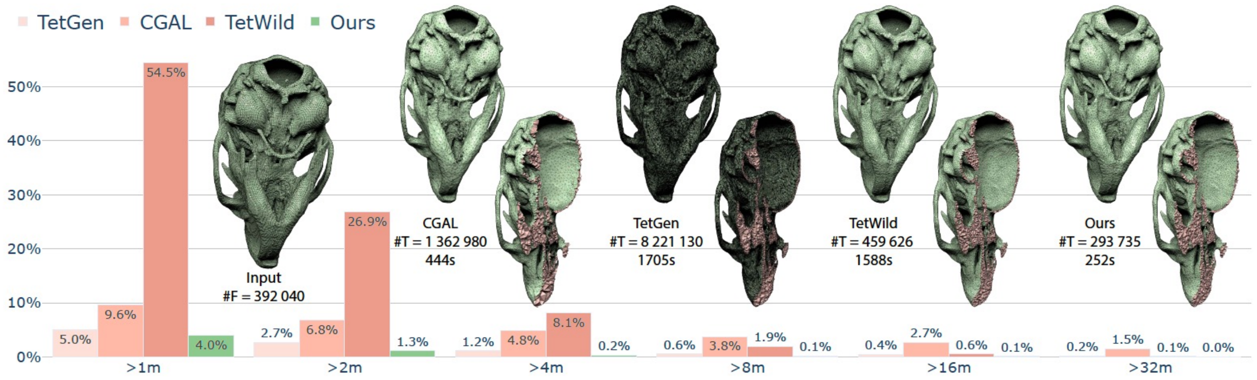

CDFEM

A verified conformal decomposition finite element method for implicit, many-material geometries

Scott A. Roberts*, Hector Mendoza, Victor E. Brunini, David R. Noble

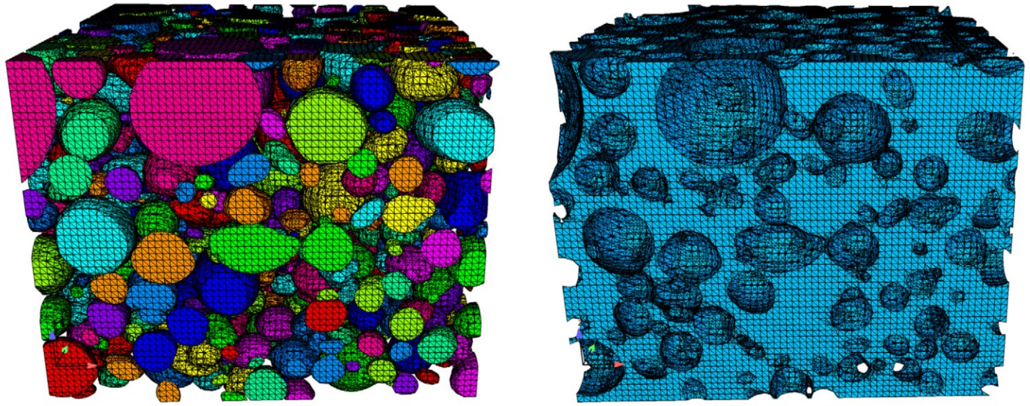

(a) Particles (b) Electrolyte

Moving Least Squares (Reproducing Kernel)

The MLS shape functions $\phi_I(\mathbf{X})$ are defined as a spatial modulation of the nodal weight functions.

$$\phi_I(\mathbf{X}) = c_I(\mathbf{X}) w_I(\mathbf{X})$$

where the modulation function $c_I(\mathbf{X})$ is found through a least square minimization process resulting in

$$c_I(\mathbf{X}) = \mathbf{g}^{\mathrm{T}}(\mathbf{X})\mathbf{A}^{-1}(\mathbf{X})\mathbf{g}(\mathbf{X}_I)$$

where

$$\mathbf{A}(\mathbf{X}) = \sum_{I \in \mathcal{N}} w_I(\mathbf{X})\mathbf{g}(\mathbf{X}_I)\mathbf{g}^{\mathrm{T}}(\mathbf{X}_I) \quad \text{(sum over neighbors)}$$

$$\mathbf{g}^{\mathrm{T}}(\mathbf{X}) = \{\, 1 \; X_1 \; X_2 \,\} \quad \text{(linear reproducibility)}$$

$$\boxed{\begin{aligned} \sum_I \phi_I(\mathbf{X}) &= 1 \\ \sum_I \mathbf{X}_I \, \phi_I(\mathbf{X}) &= \mathbf{X} \end{aligned}}$$

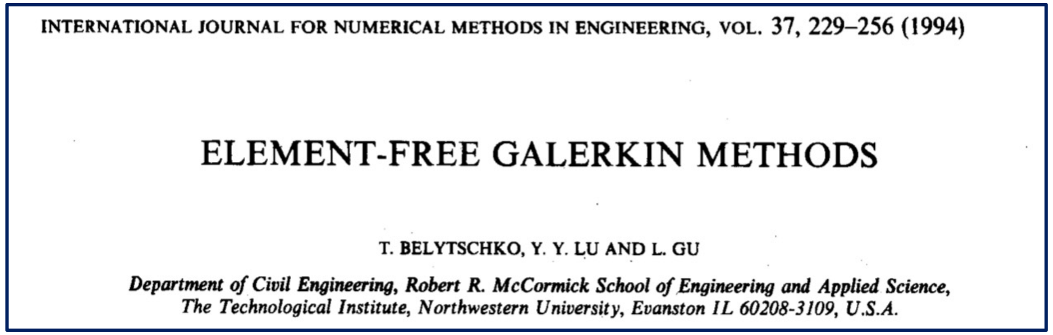

INTERNATIONAL JOURNAL FOR NUMERICAL METHODS IN ENGINEERING, VOL. 37, 229–256 (1994)

ELEMENT-FREE GALERKIN METHODS

T. BELYTSCHKO, Y. Y. LU AND L. GU

Department of Civil Engineering, Robert R. McCormick School of Engineering and Applied Science, The Technological Institute, Northwestern University, Evanston IL 60208-3109, U.S.A.

nodal weight function

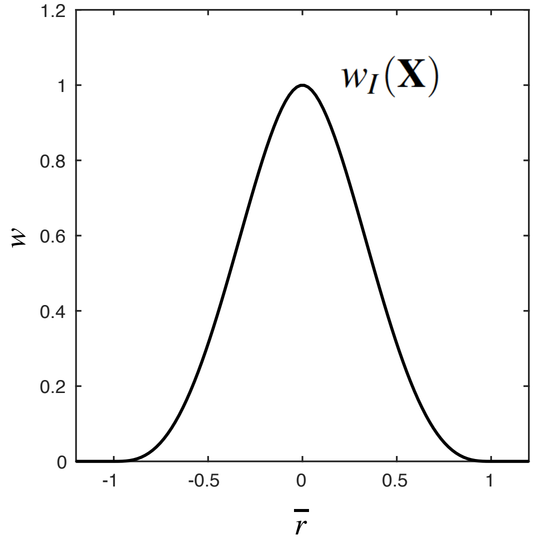

circular or rectangular support

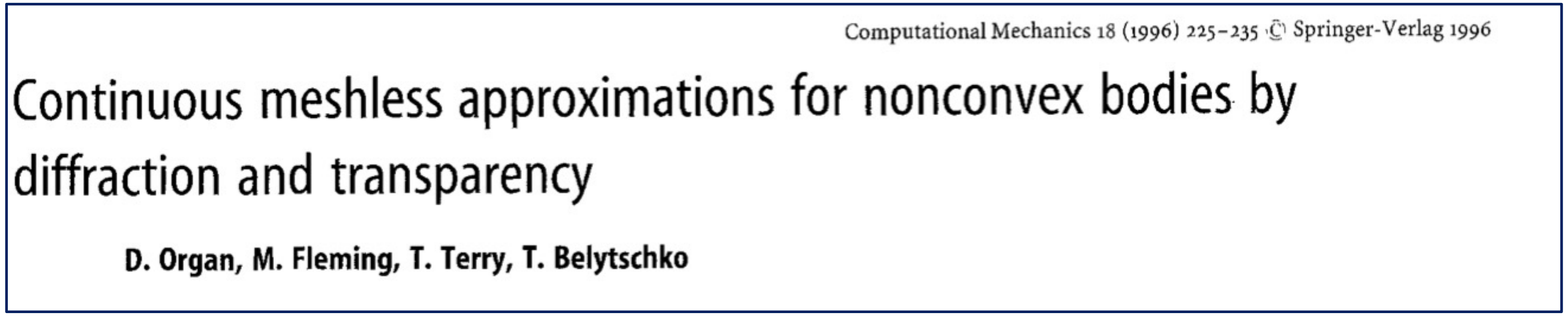

Computational Mechanics 18 (1996) 225–235 © Springer-Verlag 1996

Continuous meshless approximations for nonconvex bodies by diffraction and transparency

D. Organ, M. Fleming, T. Terry, T. Belytschko

domain
with slot

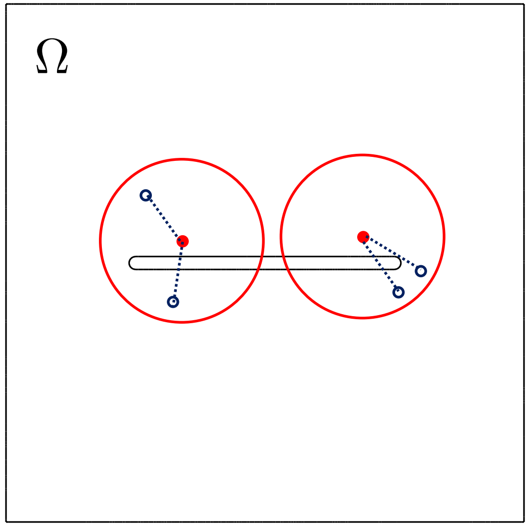

visibility criterion

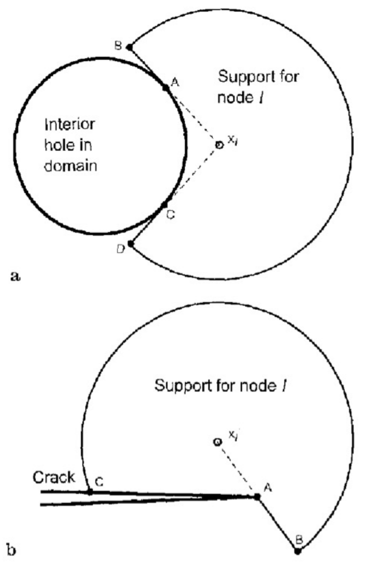

Fig. 1a,b. Domains of influence near nonconvex boundaries using the *visibility criterion* a Supportnear a hole, b Support near a crack tip

visibility criterion

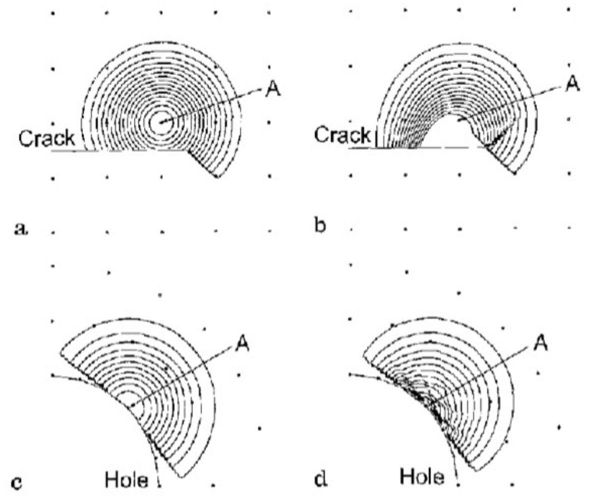

Fig. 2a–d. Contours for weight and shape functions associated with node A constructed using the *visibility criterion*. **a** Weight function near a crack tip, **b** Shape function near a crack tip, **c** Weight function near a hole, **d** Shape function near a hole

All these methods (visibility, transparency, diffraction) require use of computational geometry.

Manifold geodesic

Geodesic: path that provides the shortest distance along a manifold

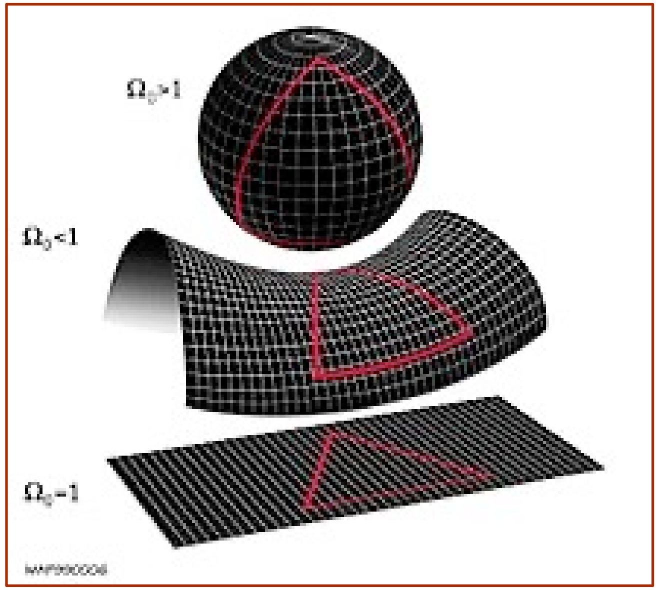

https://en.wikipedia.org/wiki/Geodesic

Euclidean manifold with boundary

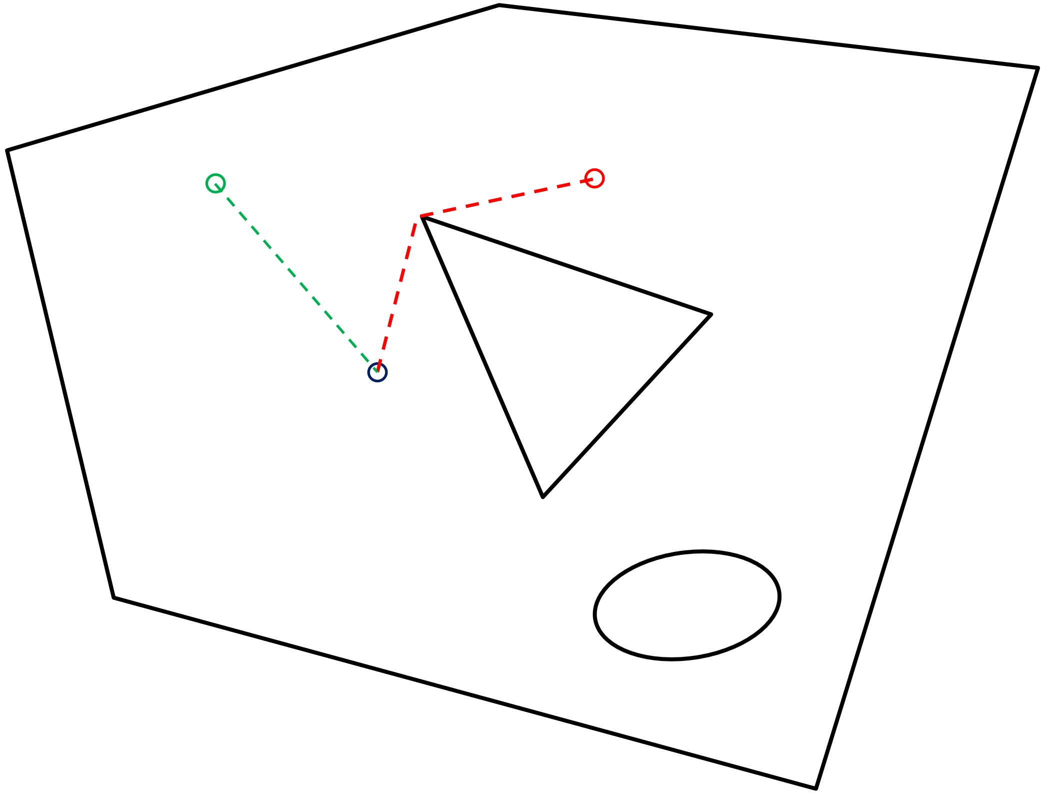

Geodesics in Heat: A New Approach to Computing Distance Based on Heat Flow

KEENAN CRANE
Caltech
and
CLARISSE WEISCHEDEL and MAX WARDETZKY,
University of Göttingen

ACM Trans. Graph. 2013 Vol. 32 Issue 5 Pages Article 152

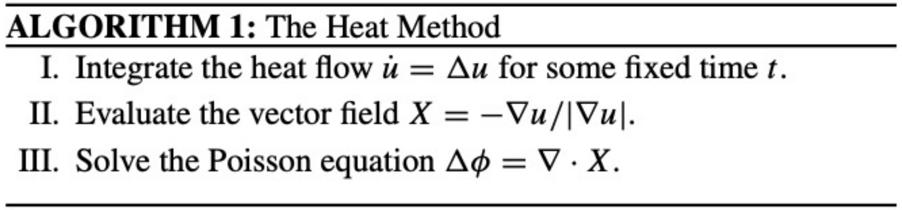

ALGORITHM 1: The Heat Method

```
I.   Integrate the heat flow $\dot{u} = \Delta u$ for some fixed time $t$.
II.  Evaluate the vector field $X = -\nabla u/|\nabla u|$.
III. Solve the Poisson equation $\Delta\phi = \nabla \cdot X$.
```

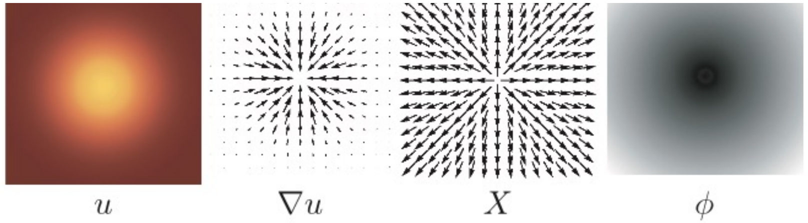

Fig. 5. Outline of the heat method. (I) Heat u is allowed to diffuse for a brief period of time *(left)*. (II) The temperature gradient ∇u *(center left)* is normalized and negated to get a unit vector field X *(center right)* pointing along geodesics. (III) A function ϕ whose gradient follows X recovers the final distance *(right)*.

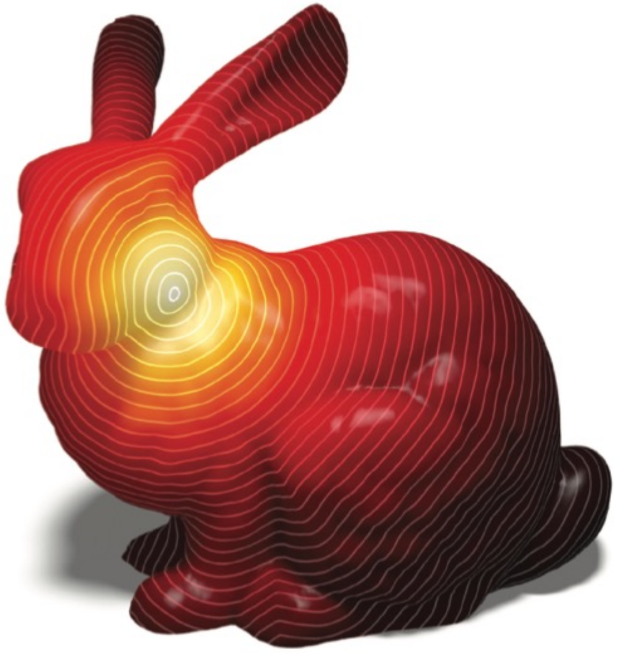

Fig. 1. Geodesic distance from a single point on a surface. The heat method allows distance to be rapidly updated for new source points or curves.

Weight functions using heat flow

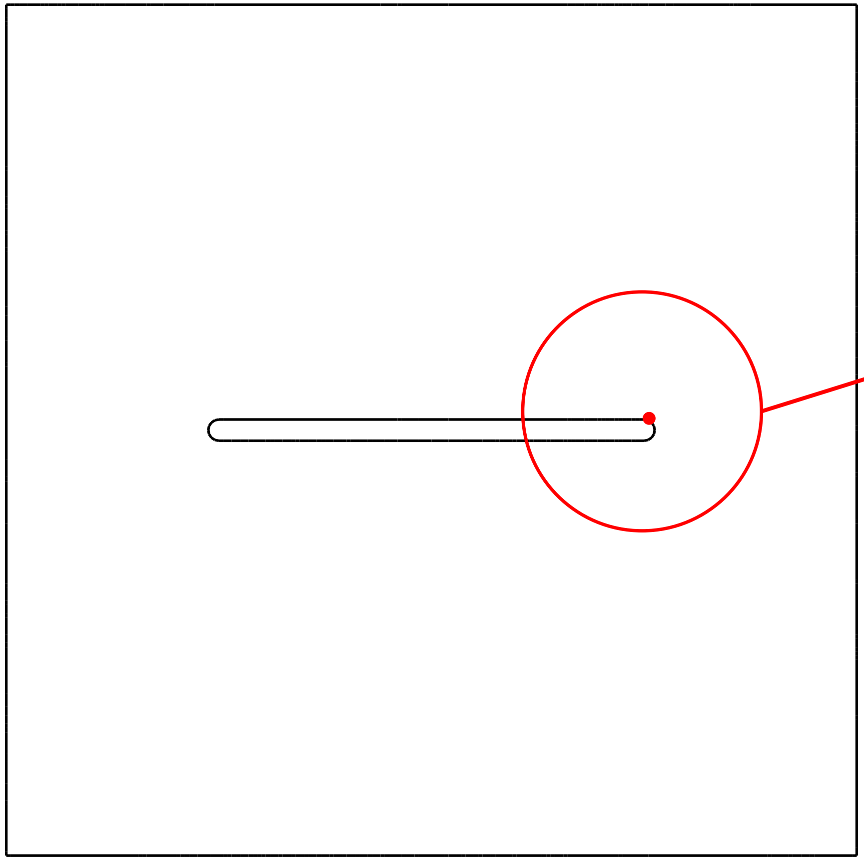

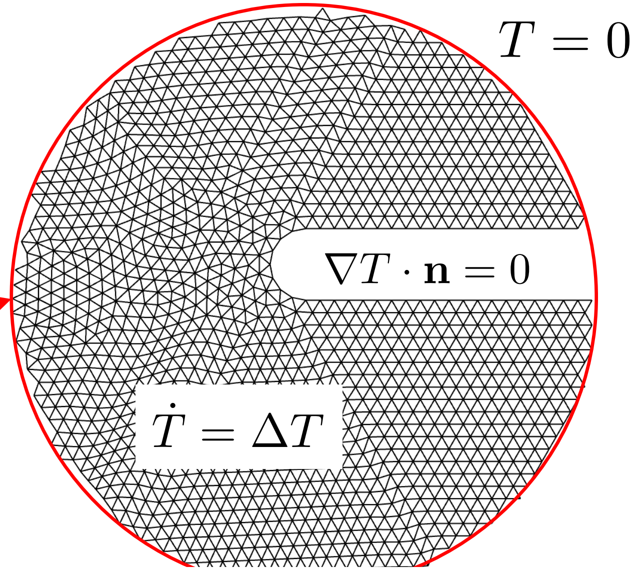

- Solve local transient heat conduction problem with certain I.C. and B.C.
- Uses local tri-mesh within support radius.

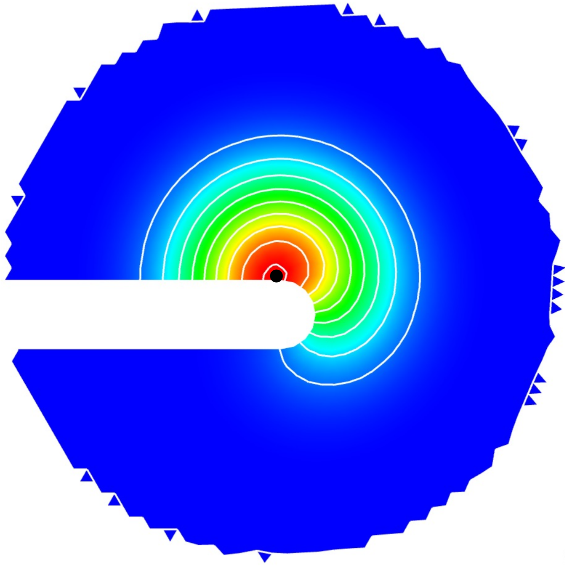

Weight functions using heat flow

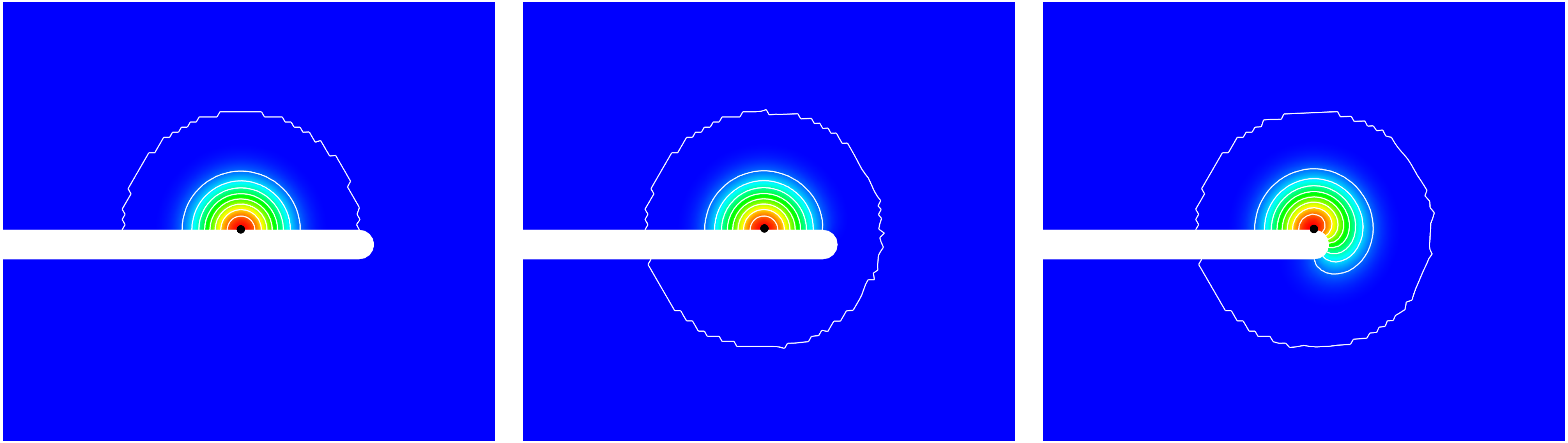

Node placement

- uniform on boundary
- random close packing on interior (maximal Poisson sampling)

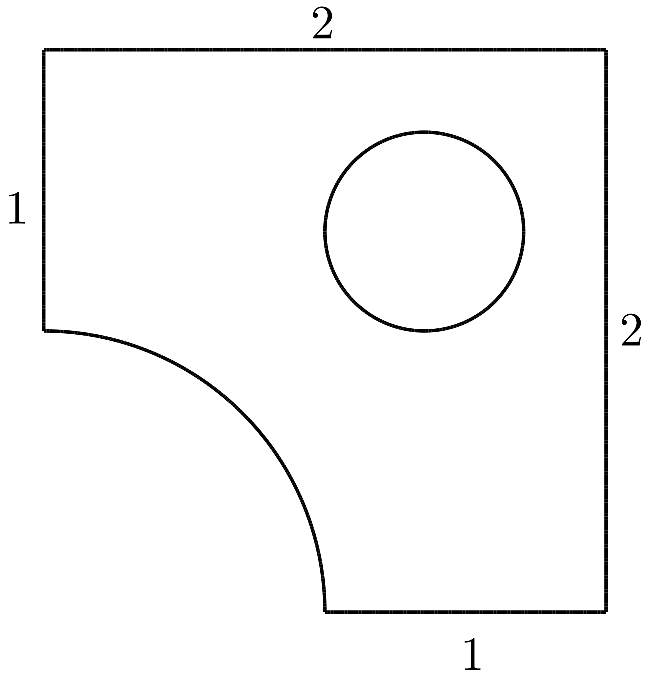

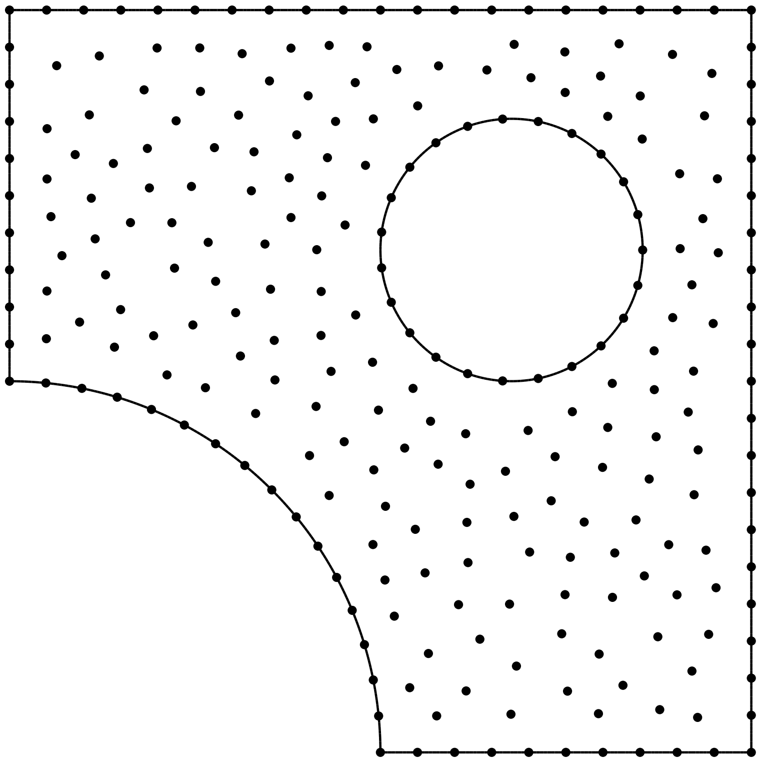

packing size:

$$H = 0.1$$

Weight function support size

support size

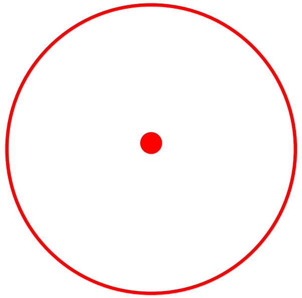

encloses underlying tri mesh

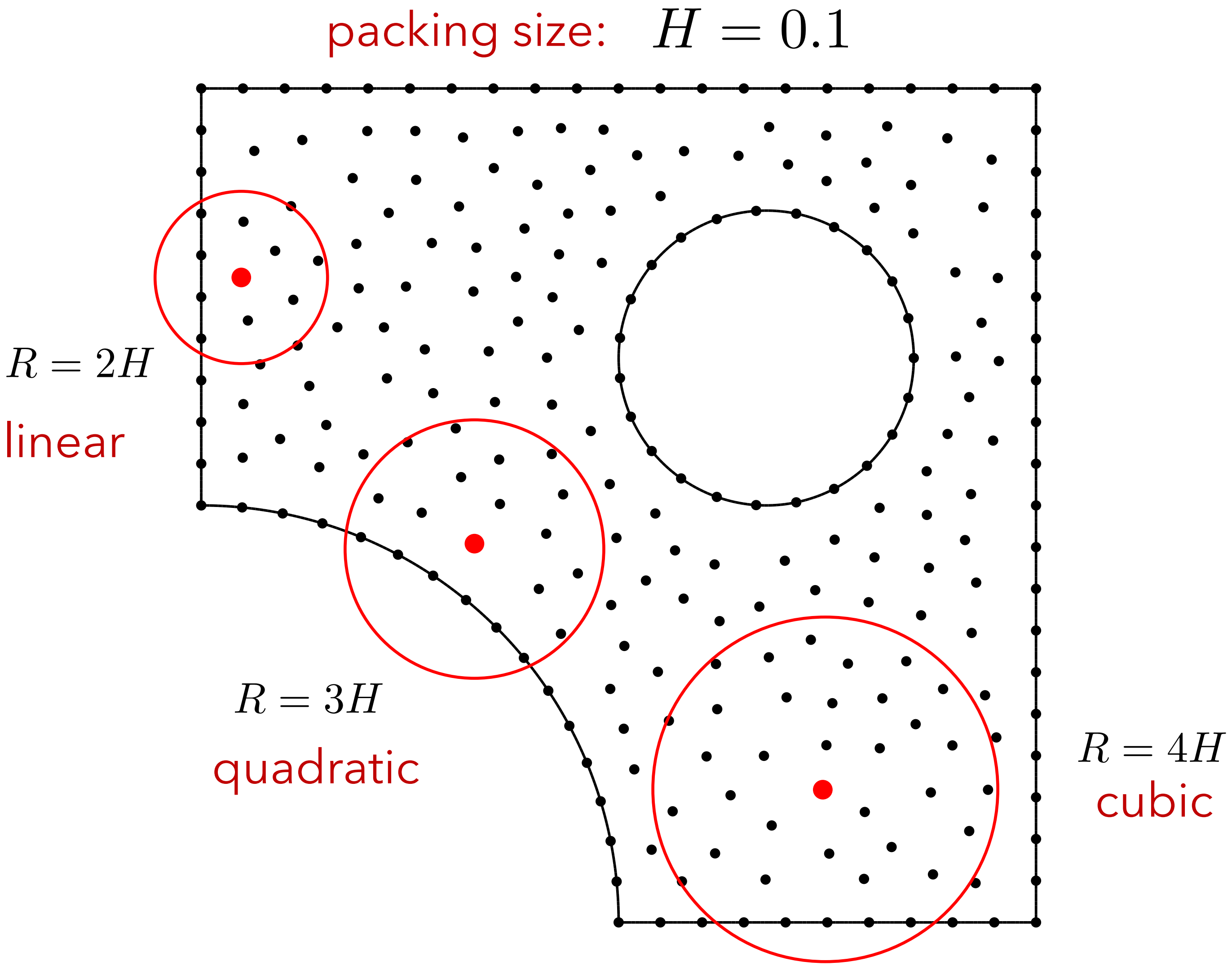

weight functions

shape functions (basis)

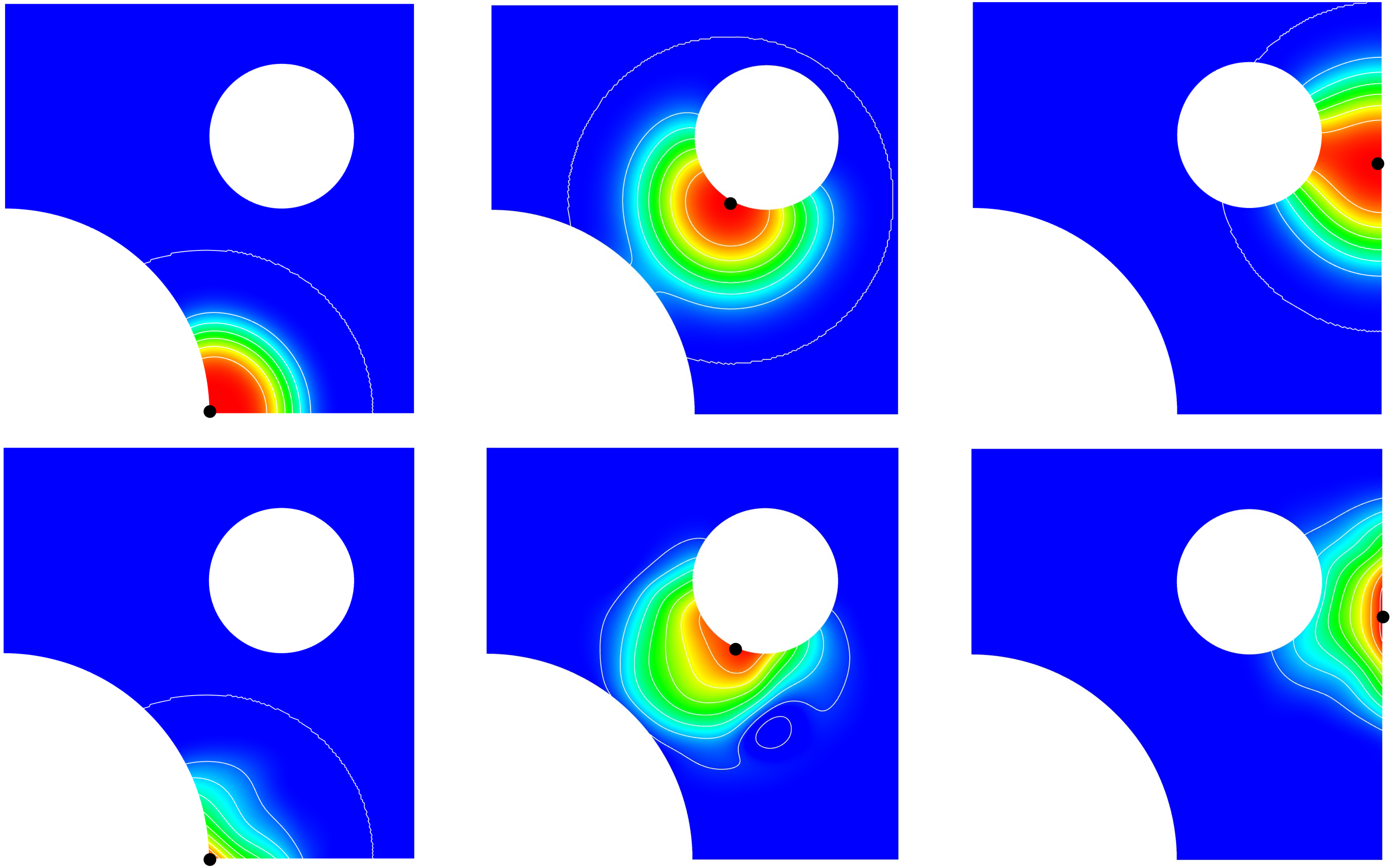

Governing equations for solid mechanics (Lagrangian)

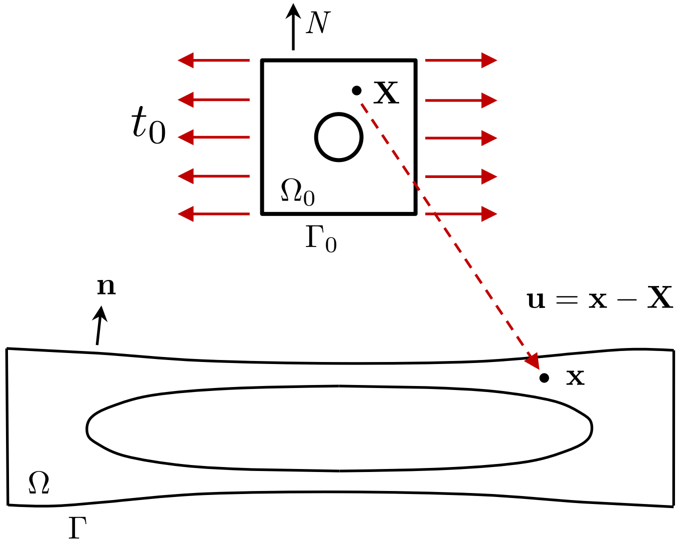

strong form

$$\frac{\partial \boldsymbol{P}}{\partial \boldsymbol{X}} : \boldsymbol{I} = \rho_0\, \ddot{\mathbf{u}}$$

$$\boldsymbol{u} = \overline{\boldsymbol{u}} \quad \text{on} \quad \Gamma_0^u \quad \text{and} \quad \boldsymbol{P} \cdot \boldsymbol{N} = \boldsymbol{t}_0 \quad \text{on} \quad \Gamma_0^t$$

P is first Piola-Kirchhoff stress tensor

weak form

find the trial functions $\boldsymbol{u} \in \boldsymbol{H}^1(\Omega_0)$ such that

$$\int_{\Gamma_0^t} \boldsymbol{t}_0 \cdot \boldsymbol{v}\, dS - \int_{\Omega_0} \boldsymbol{P} : (\partial \boldsymbol{v} / \partial \boldsymbol{X})\, d\boldsymbol{X} = \int_{\Omega_0} \rho_0\, \ddot{\mathbf{u}} \cdot \boldsymbol{v}\, d\boldsymbol{X}$$

for all test functions $\boldsymbol{v} \in \boldsymbol{H}_0^1(\Omega_0)$

Governing equations for linear elasticity

strong form $$\frac{\partial \boldsymbol{\sigma}}{\partial \mathbf{x}} : \mathbf{I} + \mathbf{f} = \mathbf{0} \qquad \mathbf{u} = \overline{\mathbf{u}} \ \text{ on } \ \Gamma_{\mathrm{u}} \ \text{ and } \ \boldsymbol{\sigma}\,\mathbf{n} = \mathbf{t} \ \text{ on } \ \Gamma_{\mathrm{t}}$$

$$\boldsymbol{\sigma} = \mathbb{C}\,\boldsymbol{\epsilon}, \text{ where } \boldsymbol{\epsilon} := \operatorname{sym}(\nabla \mathbf{u})$$ *(linear elastic)*

$$\exists\ \alpha_l\,,\ \alpha_u > 0 \ \text{ such that } \ \alpha_l\,\boldsymbol{\epsilon} : \boldsymbol{\epsilon} \le \boldsymbol{\epsilon} : (\mathbb{C}(\mathbf{x})\,\boldsymbol{\epsilon}) \le \alpha_u\,\boldsymbol{\epsilon} : \boldsymbol{\epsilon} \qquad \forall \boldsymbol{\epsilon}$$ *(uniform ellipticity)*

weak form find the trial functions $\boldsymbol{u} \in \boldsymbol{H}^1(\Omega_0)$ such that

$$\int_{\Omega} \boldsymbol{\sigma} : (\partial \mathbf{v}/\partial \mathbf{x})\, d\Omega = \int_{\Omega} \mathbf{f} \cdot \mathbf{v}\, d\Omega + \int_{\Gamma_{\mathrm{t}}} \mathbf{t} \cdot \mathbf{v}\, d\Gamma$$

for all test functions $\boldsymbol{v} \in \boldsymbol{H}_0^1(\Omega_0)$

abstract variational problem $a(u,v) = b(v)$ with bilinear form $a(u,v) = \int_{\Omega_{\mathrm{e}}} \nabla u : \mathbb{C}\, \nabla v\, d\Omega$

How to do quadrature?

Too expensive to use fine-scale triangulation for quadrature!

Observe that partition-of-unity property allows us to approximate any continuous function arbitrarily closely using only point evaluations as long as basis functions have local support.

Given $\sum_K \phi_K(\mathbf{x}) = 1$ then it follows that $f(\mathbf{x}) \approx \sum_K f(\mathbf{x}_K)\phi_K(\mathbf{x}) := f_h(\mathbf{x})$ *non-interpolatory approximation*

Theorem: For every $\varepsilon > 0$ and $\mathbf{x} \in \overline{\Omega}$, there exists $h(\varepsilon) > 0$ such that $|\, f_h(\mathbf{x}) - f(\mathbf{x})\,| < \varepsilon$.

It follows that $\int f(\mathbf{x})\, d\Omega \approx \int f_h(\mathbf{x})\, d\Omega$

with $\left| \int f_h(\mathbf{x})\, d\Omega - \int f(\mathbf{x})\, d\Omega \right| \leq \int |\, f_h(\mathbf{x}) - f(\mathbf{x})\,|\, d\Omega \leq \int \varepsilon\, d\Omega = V \cdot \varepsilon$

Can obtain rates of convergence using Taylor's theorem.

Approximation property

let $f(x) = |2x-1|\sqrt{x}$

$$f_N = \sum_{K=1}^{N} f(x_K)\phi_K(x)$$

function approximation

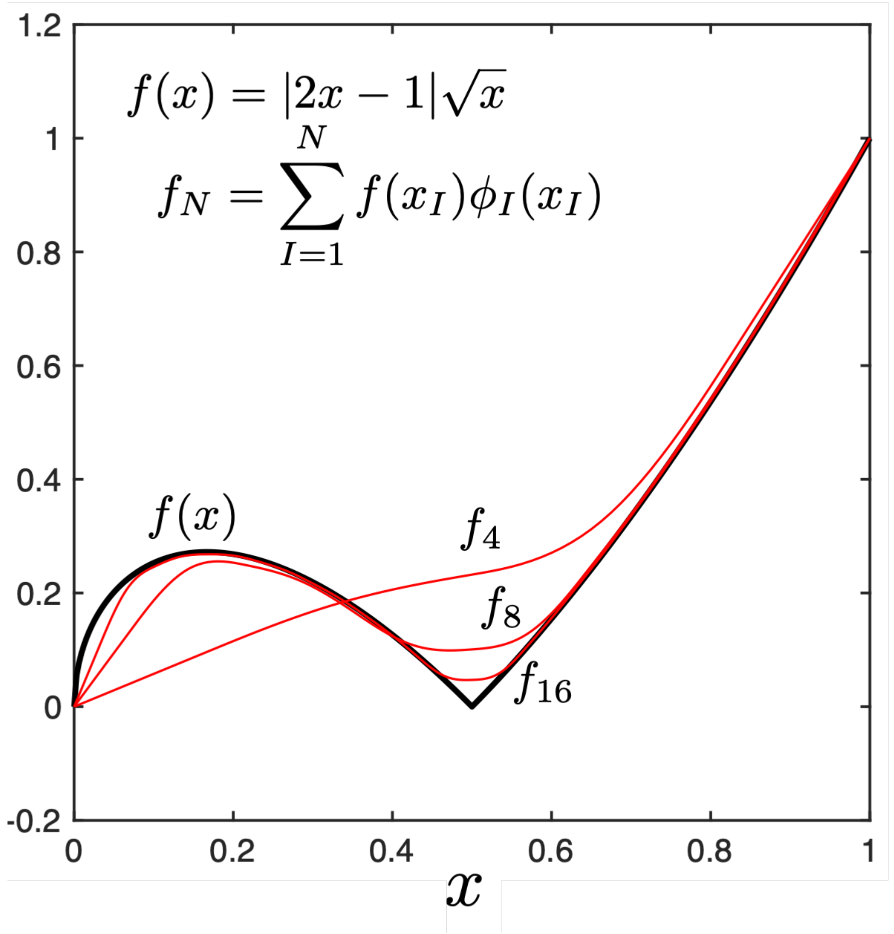

Quadrature

$$\int f(\mathbf{x})\, d\Omega \approx \int f_h(\mathbf{x})\, d\Omega = \int \sum_K f(\mathbf{x}_K)\phi_K(\mathbf{x})\, d\Omega = \sum_K f(\mathbf{x}_K) \int \phi_K(\mathbf{x})\, d\Omega$$

Define quadrature weight as $\boxed{\mathrm{w}_K = \int_\Omega \phi_K(\mathbf{x})\, d\Omega}$

$$\boxed{\int f(\mathbf{x})\, d\Omega \approx \sum_K \mathrm{w}_K f(\mathbf{x}_K)}$$

Can show that $\sum_K \mathrm{w}_K = V$ and $\sum_K \mathrm{w}_K\, \mathbf{x}_K = \int_\Omega \mathbf{x}\, d\Omega$

Now have a second-order integration scheme that can integrate linear functions exactly.

Quadrature example

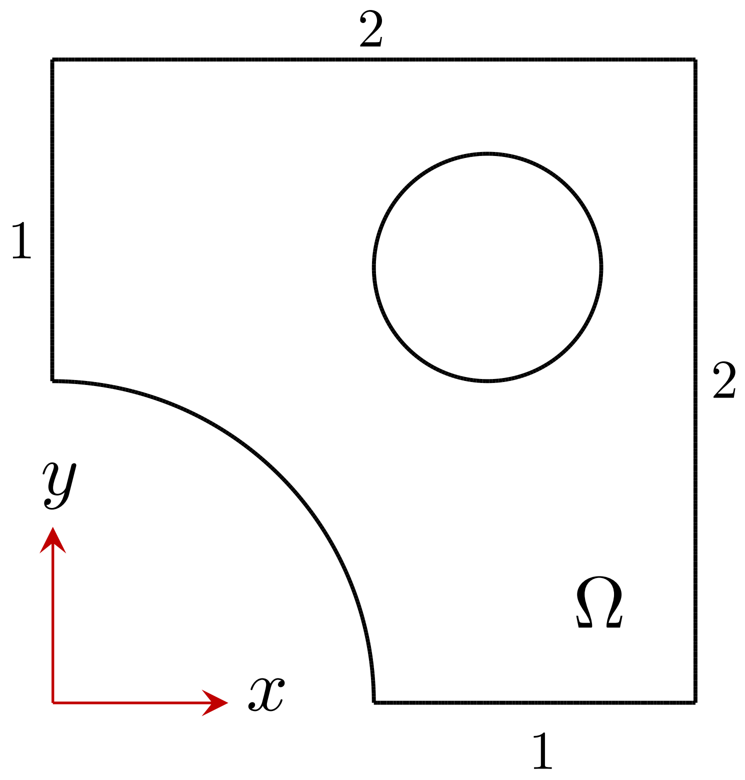

$$f(x, y) = \sin(\pi x/2)\,\sin(\pi y)$$

$$\text{error} := \left| \sum_K \mathrm{w}_K f(\mathbf{x}_K) - \int_\Omega f\, d\Omega \right|$$

Quadrature example

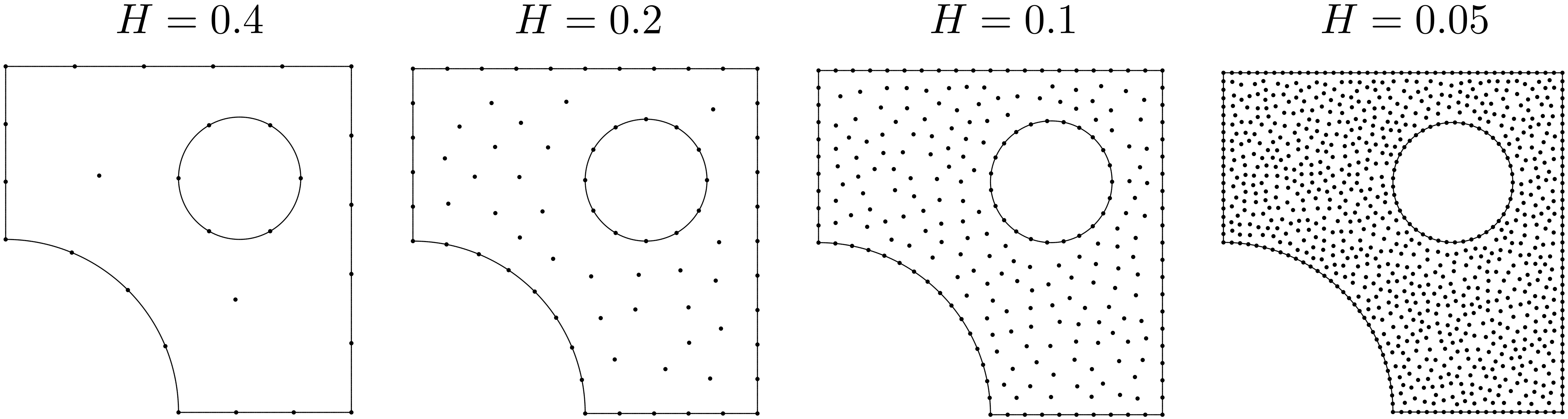

Evaluate error for 10 realizations.

Quadrature weights

$$\mathrm{w}_K = \int_\Omega \phi_K(\mathbf{x})$$

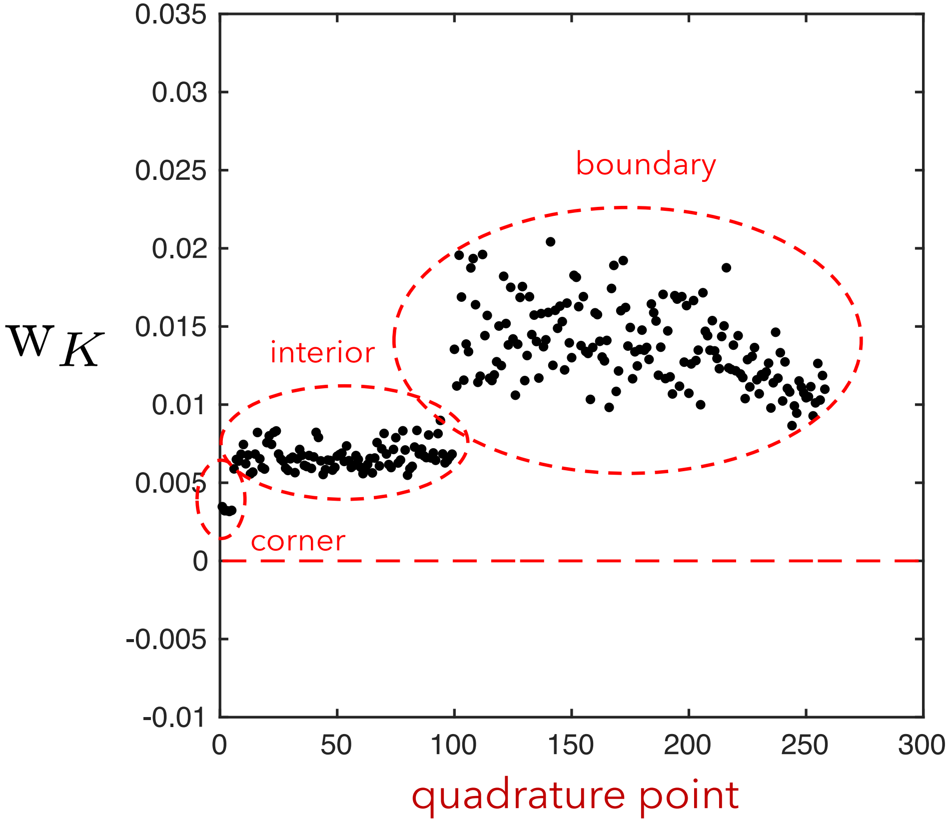

$$\text{error} := \left| \sum_K \mathrm{w}_K f(\mathbf{x}_K) - \int_\Omega f \, d\Omega \right|$$

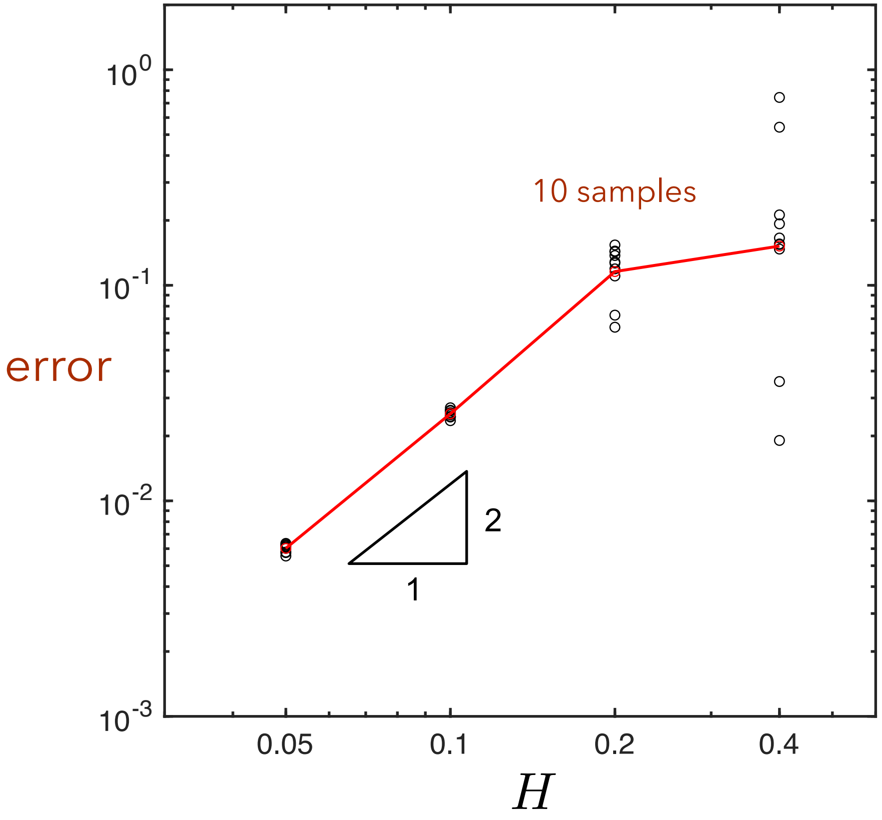

Element-free approach to solve BVPs

Use two meshfree clouds: one for solution discretization (DoF) and one for quadrature.

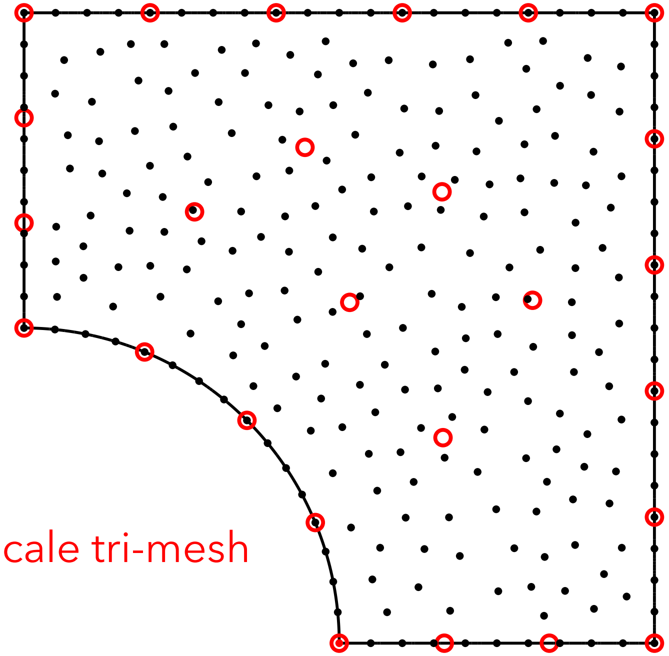

○ DoF point

● quadrature point

+ fine-scale tri-mesh

quad-to-dof ratio = 4^2

What ratio of quad points to dof points is needed for stability (coercivity of bilinear form)?

Patch test (linear consistency)

uniaxial tension

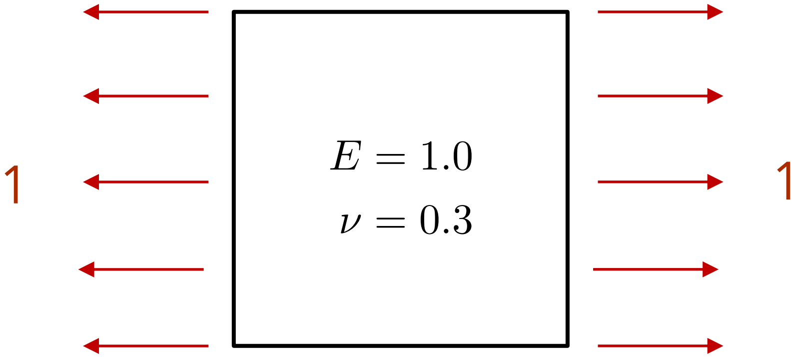

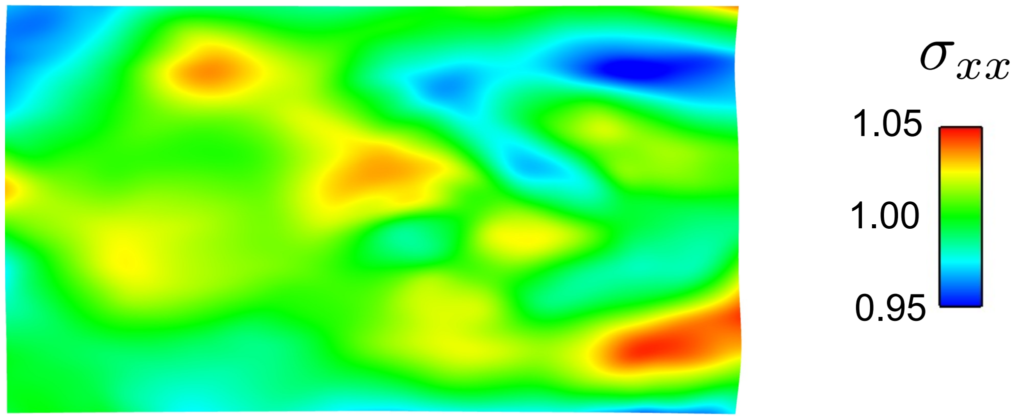

error $> 5\%$

Consistency of discrete form (integration)

- For convergence of discrete approximation, need to ensure consistency of discrete and continuous bilinear forms.
- Requires polynomial consistency of shape-function gradients (including quadrature).
- To obtain quadrature consistency, project the DoF shape function gradients to the subspace of quadrature shape functions.
- Only performed once in a pre-processing step.

$\{\phi_I, I = 1, \ldots, N\}$ *DoF basis (shape functions)*

$\{\Phi_K, K = 1, \ldots, M\}$ *Quadrature basis (shape functions)*

$$\overline{\nabla}\phi_I := \arg\min \int_\Omega \left(\nabla\phi_I - \sum_{K=1}^{M} a^K \Phi_K \right)^2 d\Omega$$

(L_2 projection)

The projection can be written in terms of the dual or conjugate basis $\{\Phi^J\}$

$$(\Phi_K, \Phi^J) = \delta_K^J$$ *bi-orthogonal*

$$\overline{\nabla}\phi_I = \sum_K \underbrace{(\nabla\phi_I, \Phi_K)}_{\text{covariant components}}\Phi^K = \sum_K \underbrace{(\nabla\phi_I, \Phi^K)}_{\text{contravariant components}}\Phi_K$$

Can prove polynomial consistency up to the order of the precision of $\{\Phi_K\}$

Theorem: $\int_\Omega \mathbf{p}\,\overline{\nabla}\phi_I\,d\Omega = \int_\Omega \mathbf{p}\,\nabla\phi_I\,d\Omega$ for all $\mathbf{p} \in \mathbb{P}_k(\Omega)$

This ensures satisfaction of the patch test.

Replace the original bilinear form $a(u,v) = \int_\Omega \nabla u : \mathbb{C}\,\nabla v\, d\Omega$

with this modified bilinear form $\bar{a}(u,v) = \int_\Omega \overline{\nabla} u : \mathbb{C}\,\overline{\nabla} v\, d\Omega$

Note: This modified bilinear form is still symmetric (Bubnov-Galerkin).

$$\bar{a}(u,v) = \int_\Omega \left[\sum_I (\nabla u, \Phi_I)\Phi^I \right] \mathbb{C} \left[\sum_J (\nabla v, \Phi_J)\Phi^J \right] d\Omega$$

$$\bar{a}(u,v) = \sum_{I,J} (\nabla u, \Phi_I)\,\mathbb{C}\,(\nabla v, \Phi_J) \underbrace{\int_{\Omega_\mathrm{e}} \Phi^I \Phi^J \, d\Omega}_{G^{IJ}}$$

inverse of the Gram matrix

Can show that $G^{IJ} = (G_{IJ})^{-1}$

where $G_{IJ} = \int_{\Omega_e} \Phi_I \Phi_J \, d\Omega$ is the Gram matrix for the basis $\{\Phi_K\}$

Can show that $\Phi^I = G^{IJ}\Phi_J$ and $\Phi_I = G_{IJ}\Phi^J$

"raising" and "lowering" of indices

$$\boxed{\bar{a}(u,v) = \sum_{I,J} G^{IJ} (\nabla u, \Phi_I)\, \mathbb{C}\, (\nabla v, \Phi_J) = \sum_K (\nabla u, \Phi^K)\, \mathbb{C}\, (\nabla v, \Phi_K)}$$

$$\underbrace{\qquad\qquad\qquad\qquad\qquad\qquad}_{\text{Looks like a sum over quadrature points.}}$$

Since $G^{IJ} = (G_{IJ})^{-1}$ is dense:

Replace G_{IJ} with row-sum lumped version: $G^L_{IJ} := \sum_J G_{IJ} = \mathrm{diag}\{\mathrm{w}_K\}$

where recall $\mathrm{w}_K = \int_\Omega \phi_K(\mathbf{x})\, d\Omega$

Then $\overline{a}(u,v) \rightarrow \overline{a}^L(u,v) = \sum_K \frac{1}{\mathrm{w}_K}(\nabla u, \Phi_K)\,\mathbb{C}\,(\nabla v, \Phi_K)$ where $(G^L_{IJ})^{-1} = \mathrm{diag}\left\{\frac{1}{\mathrm{w}_K}\right\}$

Can write $\overline{a}^L(u,v)$ as $\boxed{\overline{a}^L(u,v) = \sum_K \mathrm{w}_K\,(\overline{\nabla} u)_K : \mathbb{C}\,(\overline{\nabla} v)_K}$

where $\boxed{(\overline{\nabla} u)_K := \frac{1}{\mathrm{w}_K}\int_\Omega (\nabla u)\,\Phi_K\, d\Omega}$ which has the form of a discrete derivative at a quadrature point K.

Our discrete bilinear form is now "sparse."

Patch test (linear consistency)

uniaxial tension

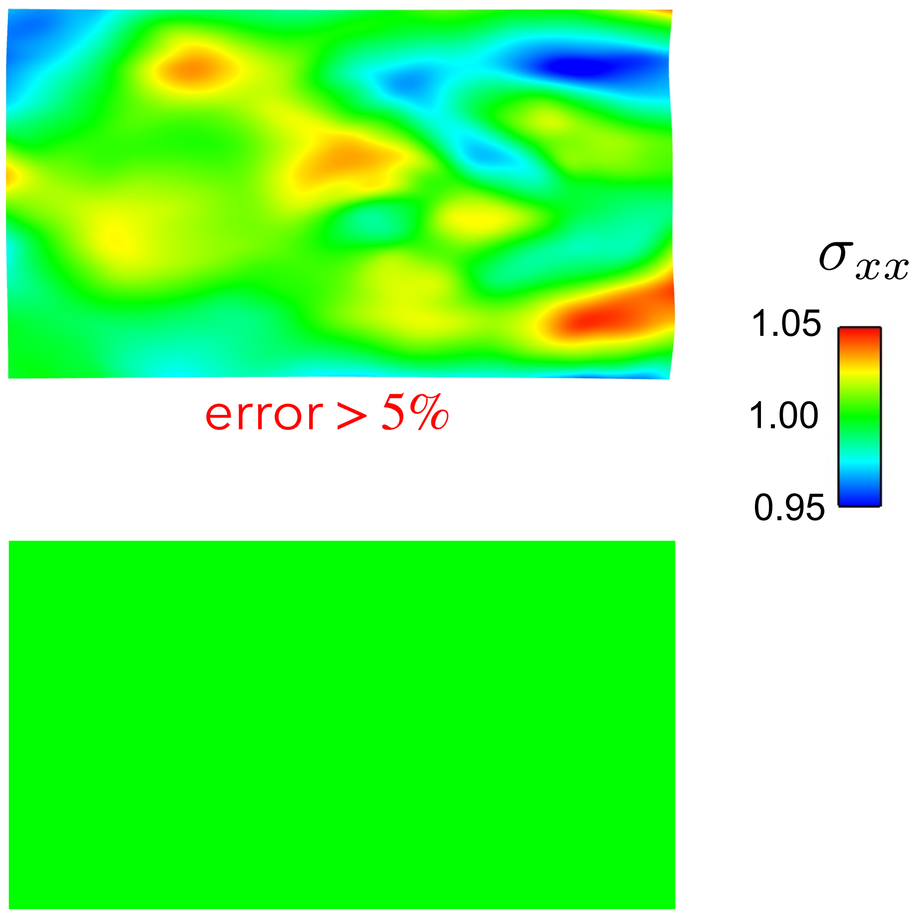

no projection

error > 5%

with projection

error < 10^{-13}

pure shear

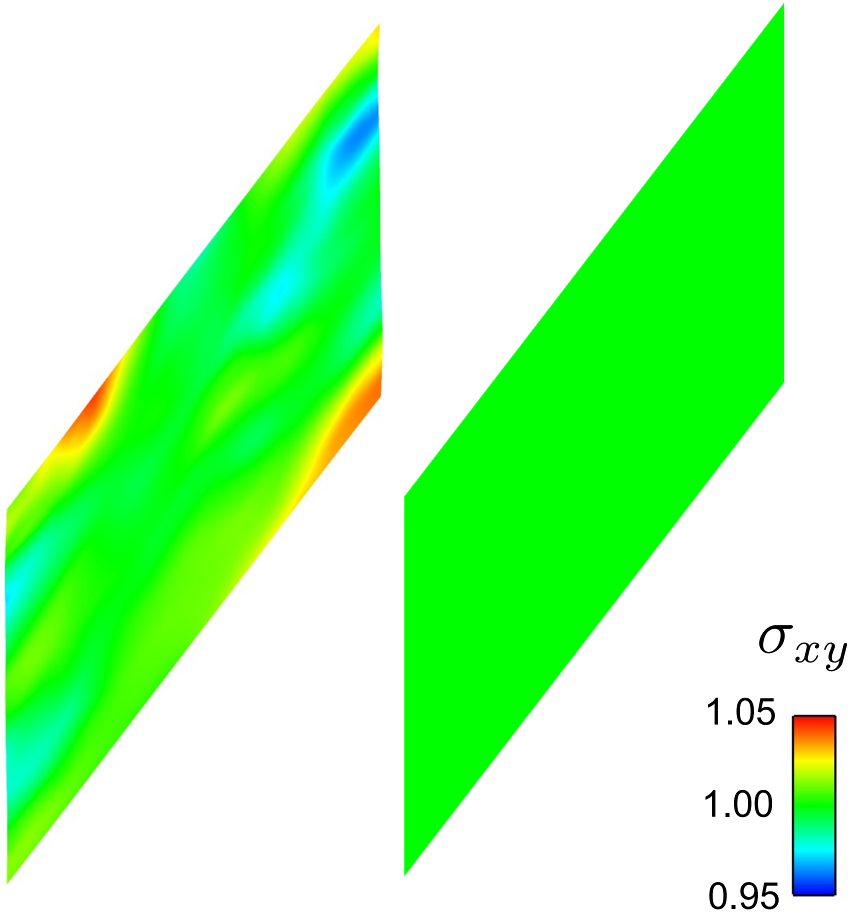

Example: plate with hole

uniaxial tension

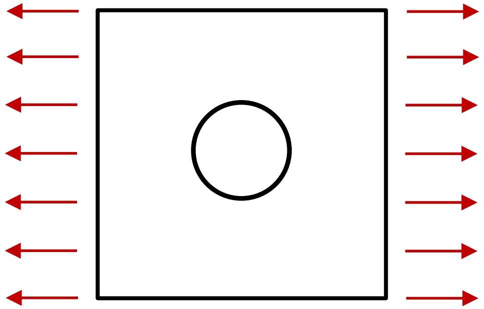

$E = 1.0$

$\nu = 0.3$

exact

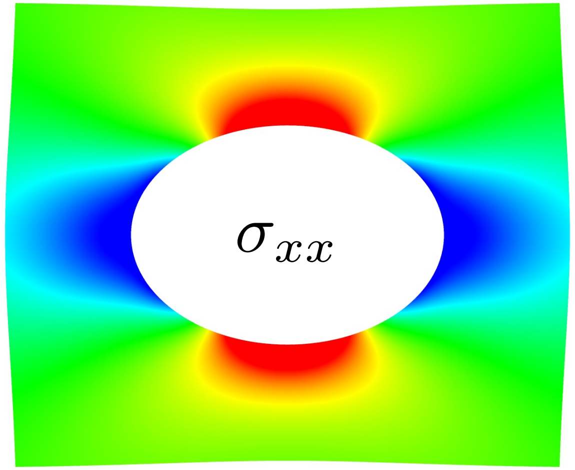

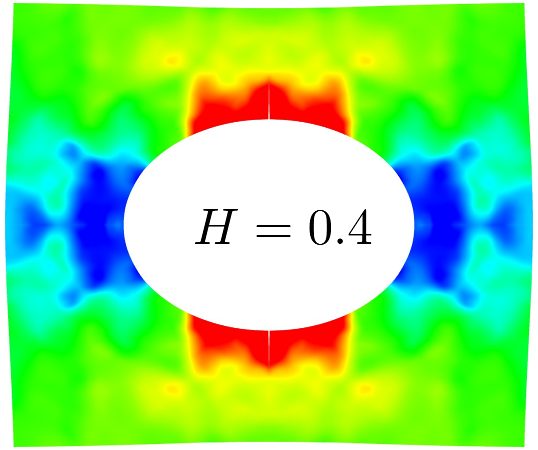

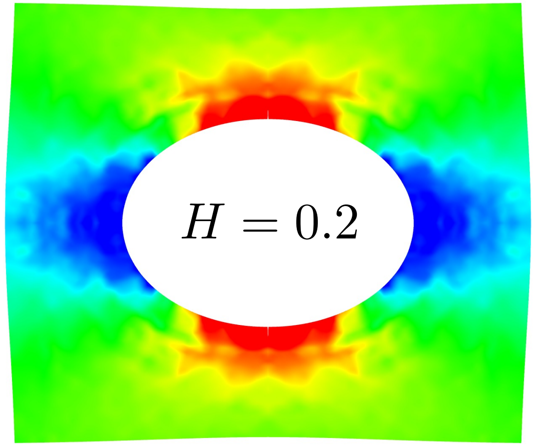

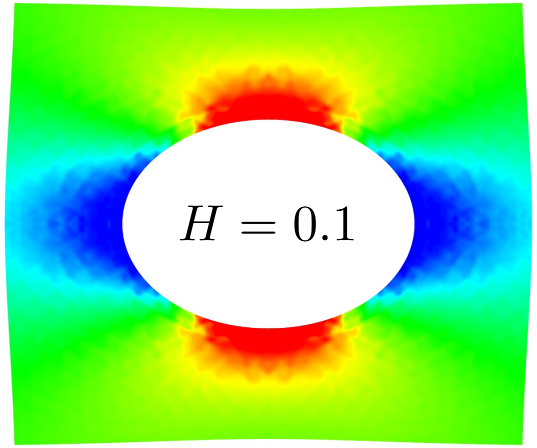

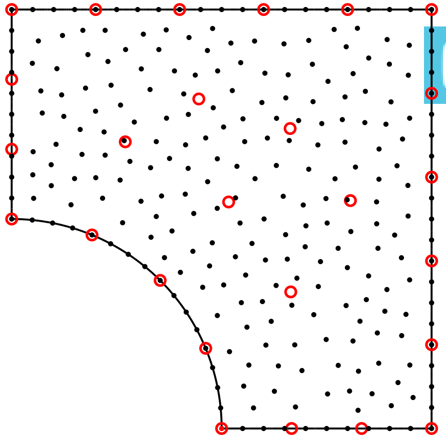

Example: plate with hole

L_2 norm

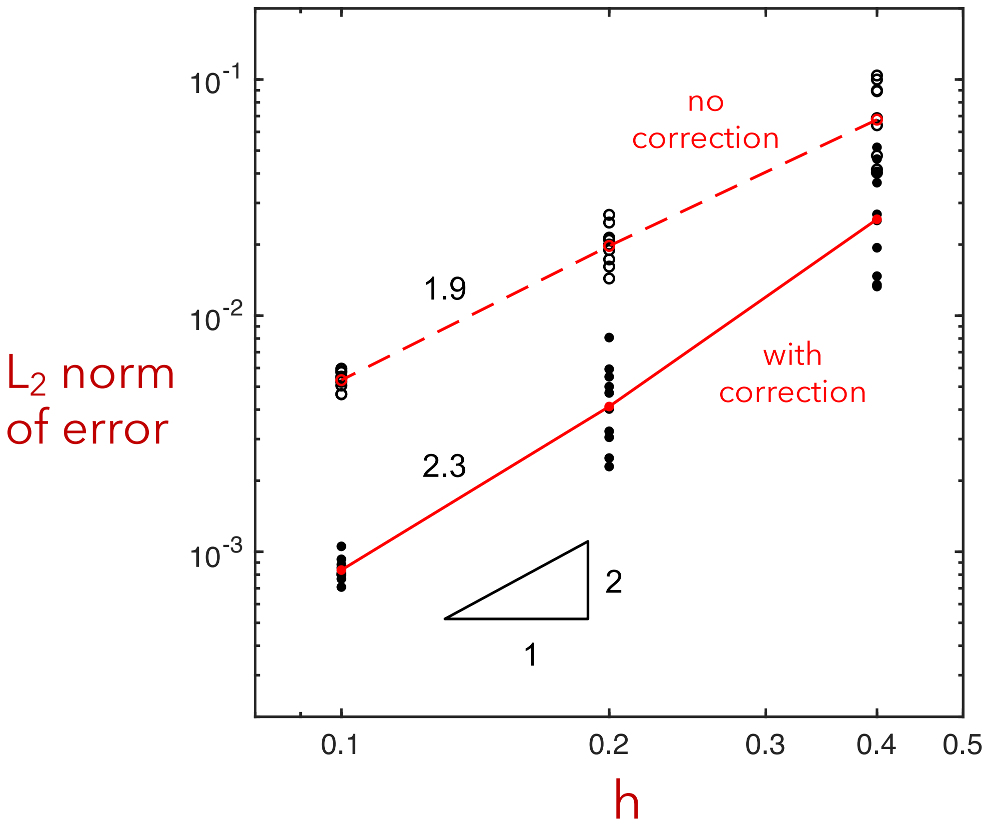

energy norm

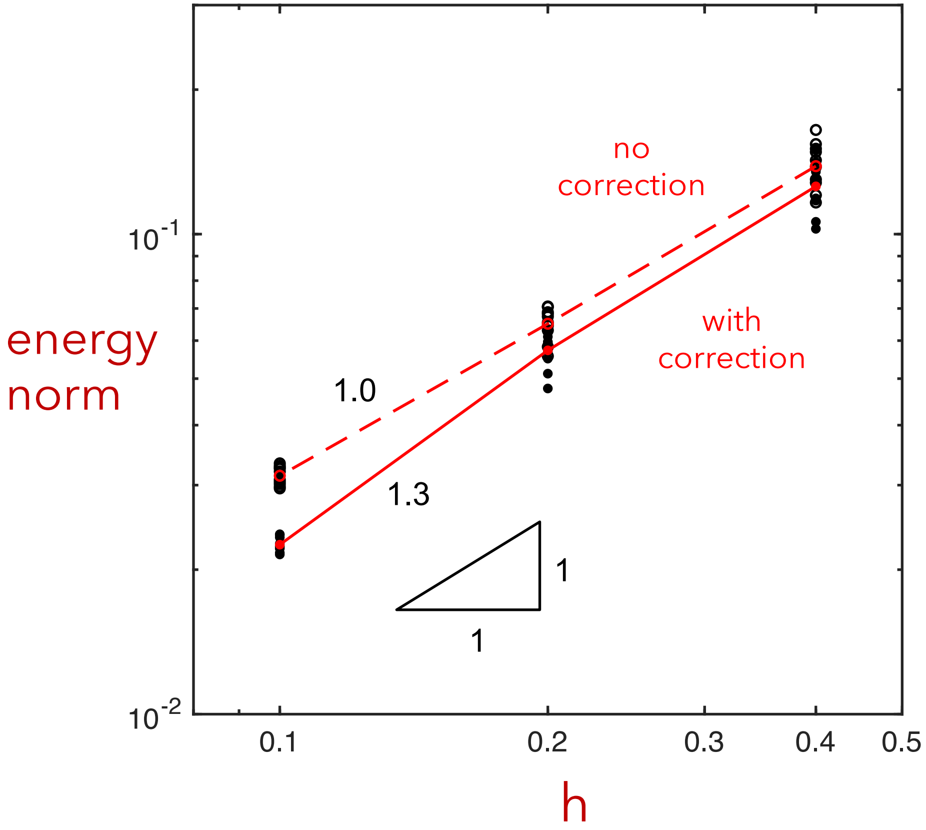

Example

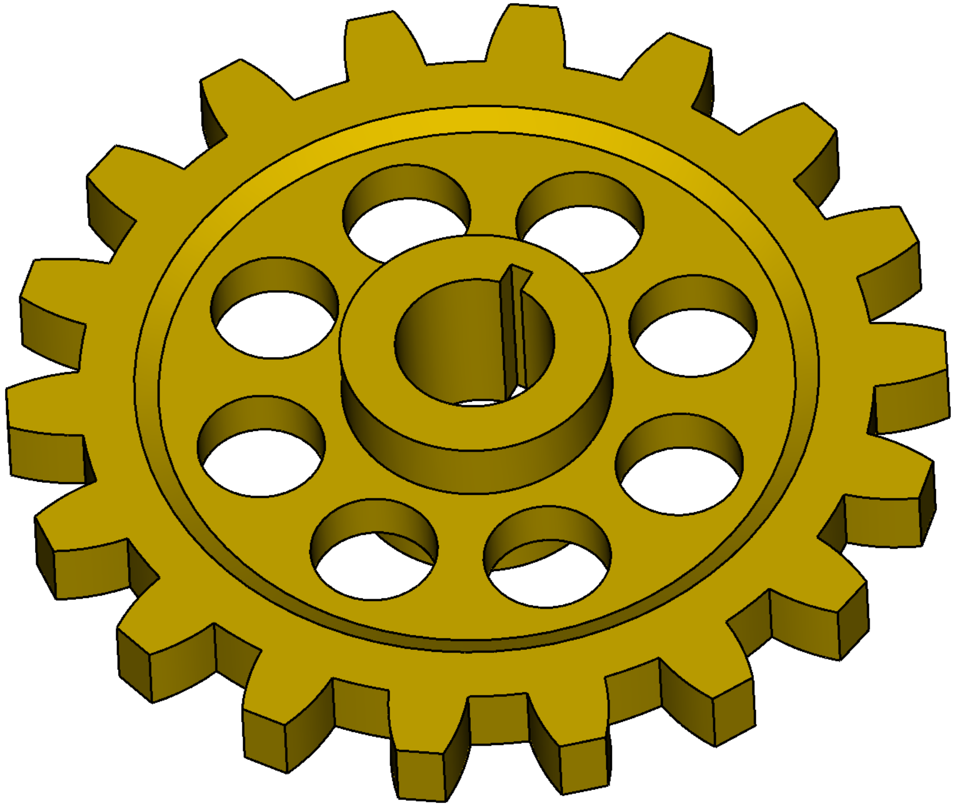

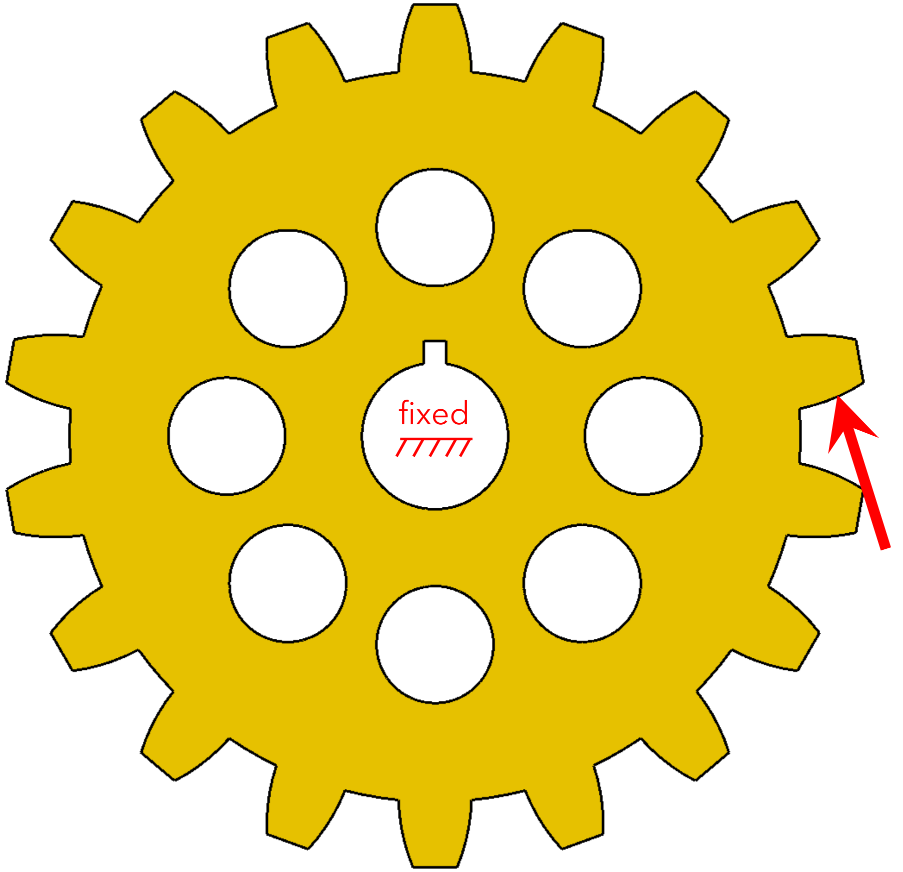

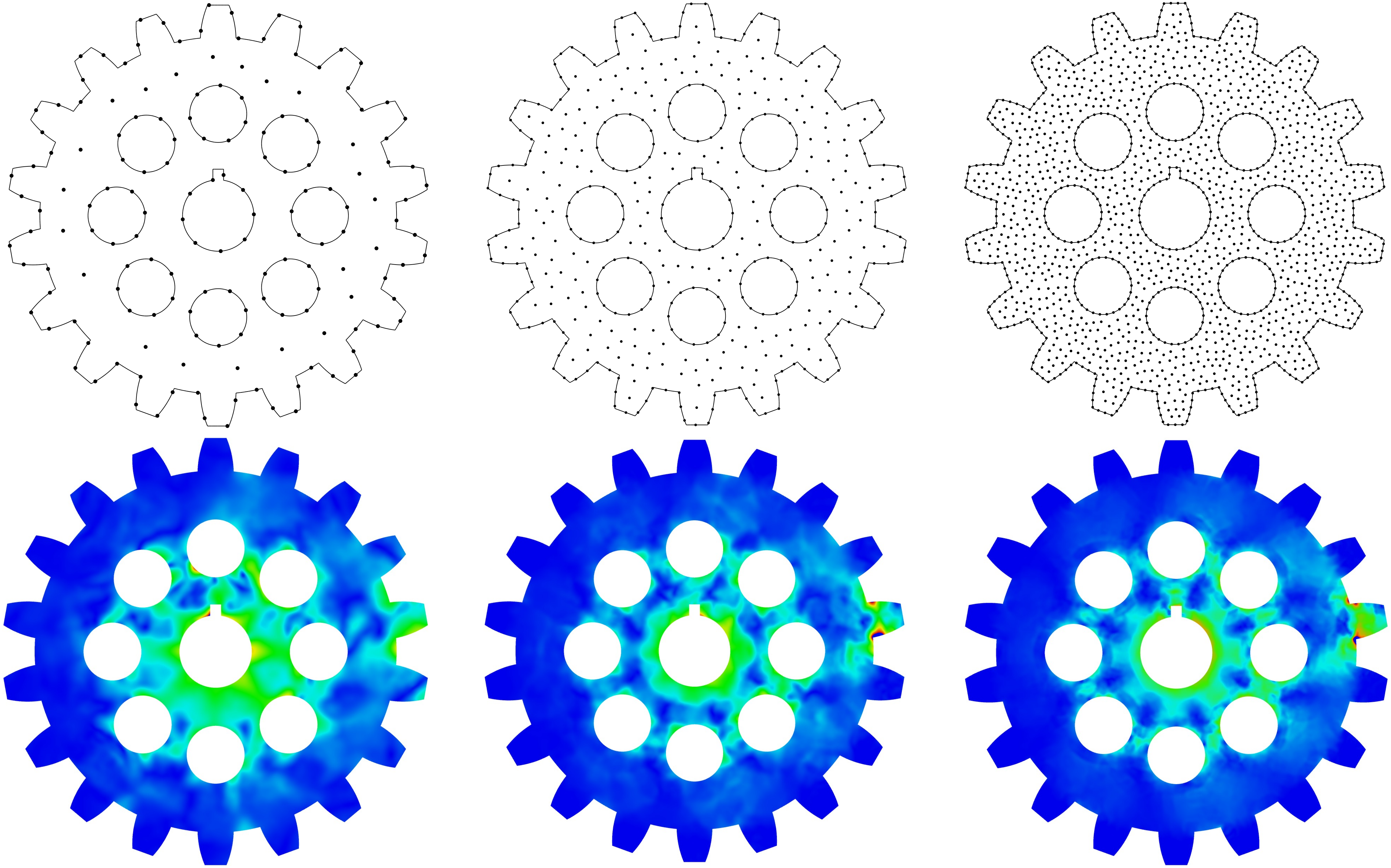

Example: hyperelastic, hole-in-plate

uniaxial extension

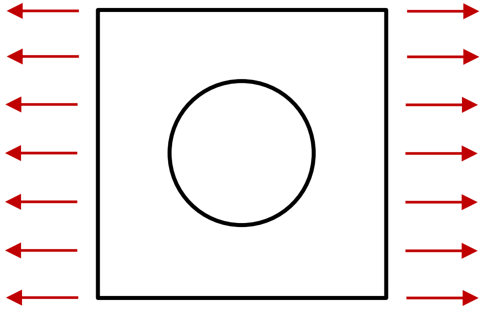

- plane strain
- quarter symmetry model used

compressible neo-Hookean material

$$\boldsymbol{\sigma} = \frac{\mu}{J}(\mathbf{F}\mathbf{F}^T - \mathbf{I}) + \frac{\lambda}{\ln J}\mathbf{I}$$

$$J = \det \mathbf{F} \qquad \mathbf{F} = \frac{\partial \mathbf{x}}{\partial \mathbf{X}}$$

quad mesh

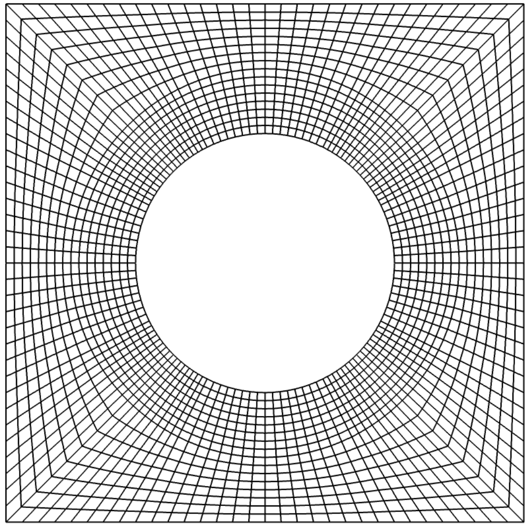

mapped hexagon mesh

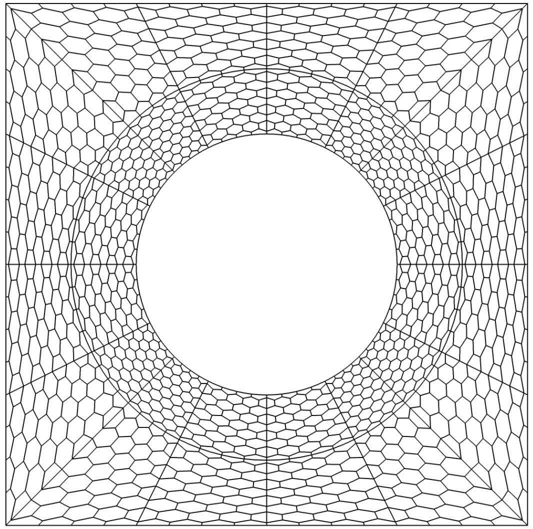

Example: hyperelastic, hole-in-plate

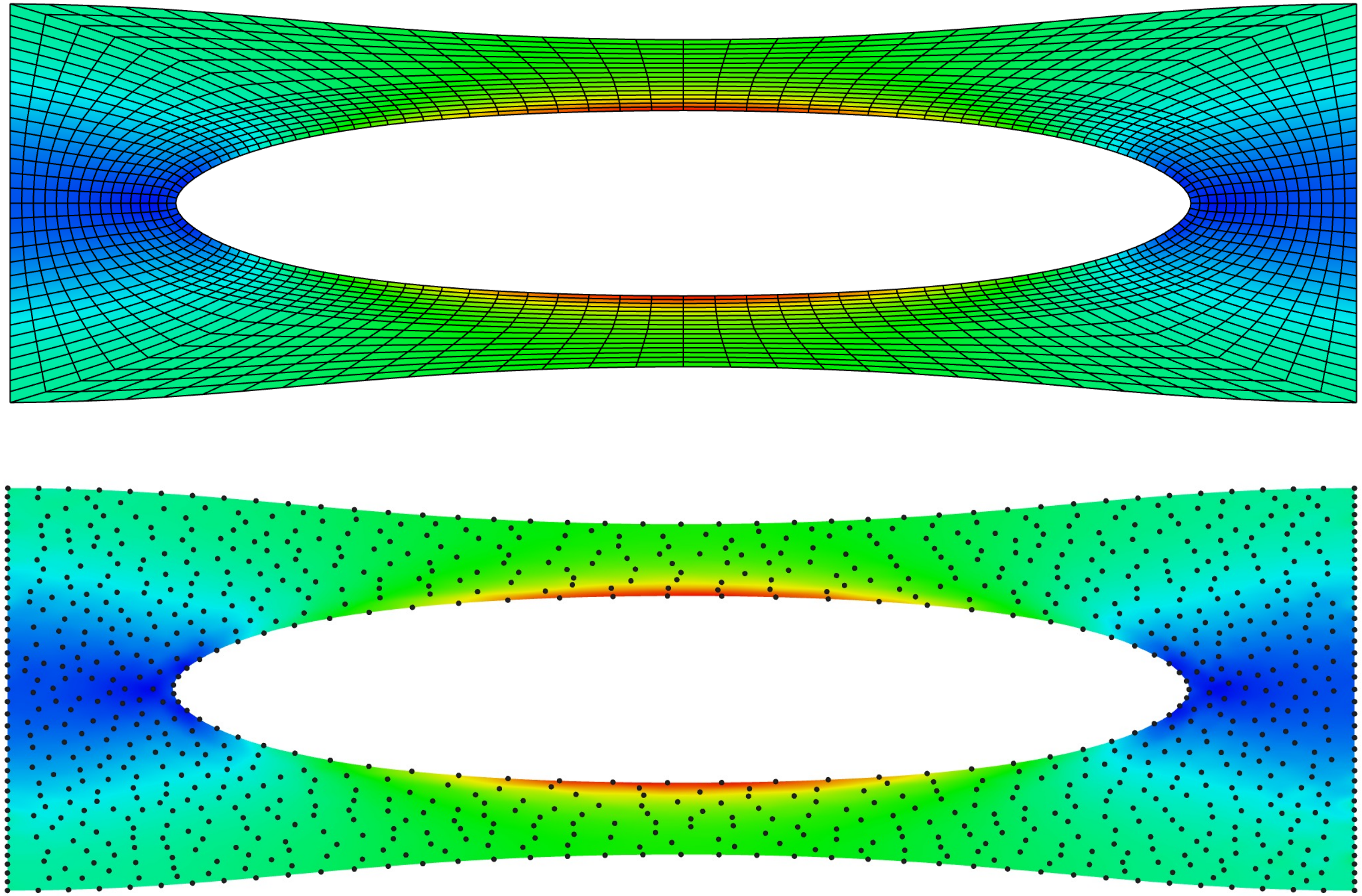

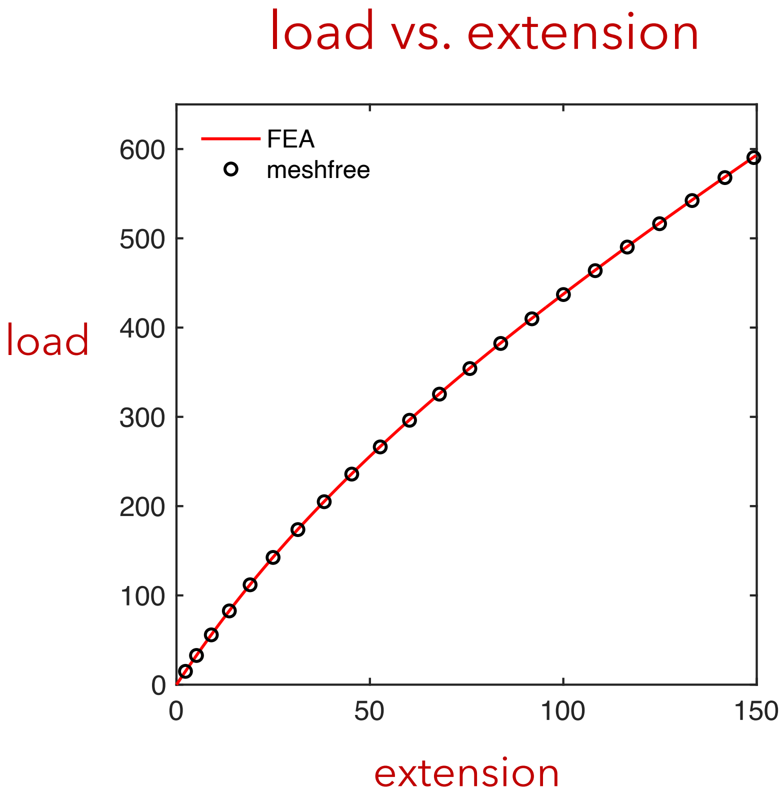

load vs. extension

Example: elastic-plastic, hole-in-plate

yield surface $f(\sigma, \bar{\varepsilon}^p) = \phi(\sigma) - \sigma_y(\bar{\varepsilon}^p) = 0$

$$\phi(\sigma) = \left\{ \frac{1}{2} \left(|\sigma_1 - \sigma_2|^2 + |\sigma_1 - \sigma_3|^2 + |\sigma_2 - \sigma_3|^2 \right) \right\}^{1/2}$$

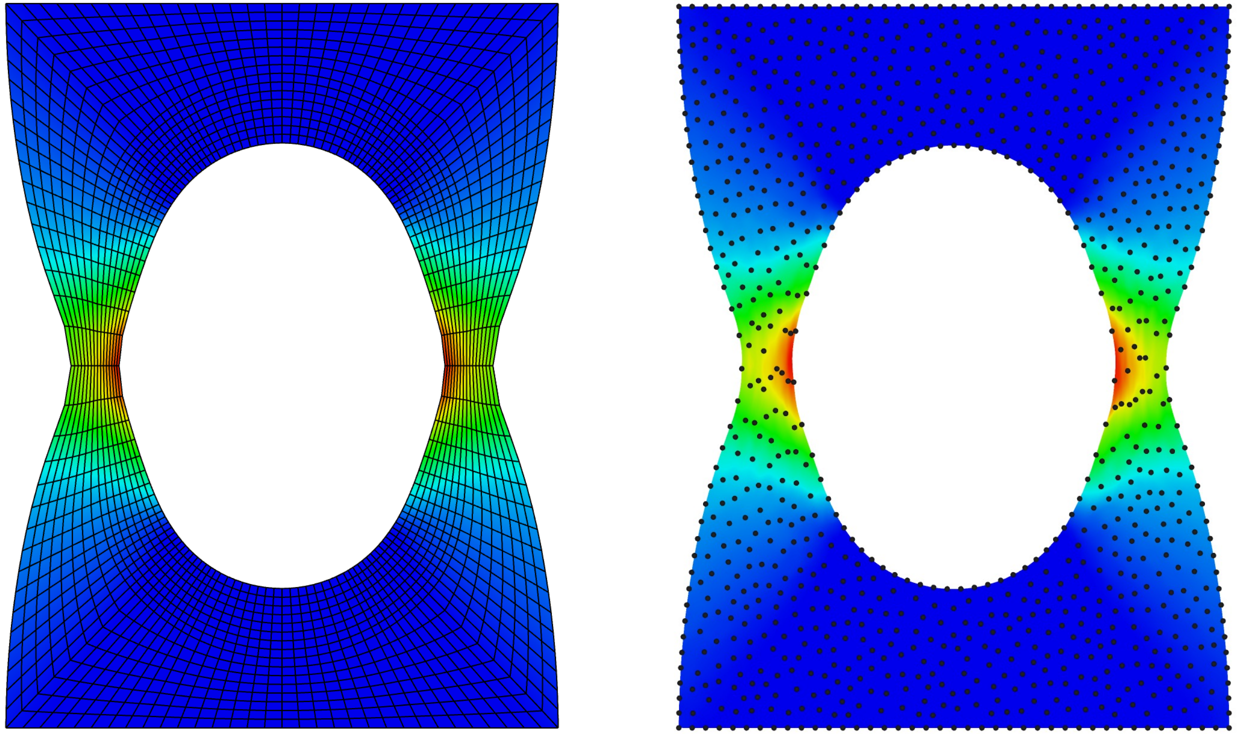

plastic strain field

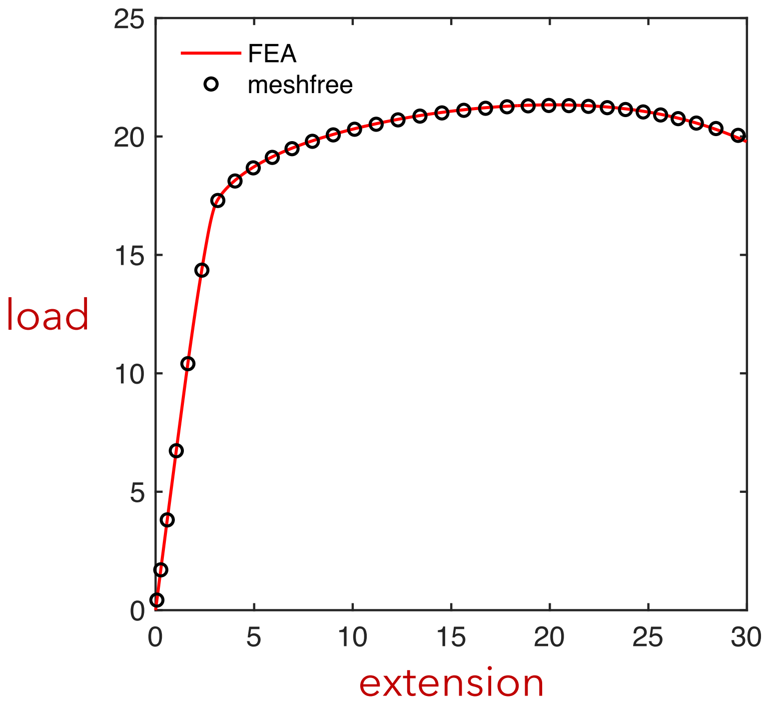

load vs. extension

Summary

1. Separate domain discretization from solution discretization (fine-scale domain triangulation with coarse-scale solution discretization).
2. Example of discretization-based reduced order model.
3. Generation of meshfree weight functions using manifold geodesics.
4. New approach to quadrature for meshfree methods based on secondary basis.
5. Projected shape-function gradients using dual basis for polynomial consistency.
6. Observed optimal convergence rates for 2D elasticity.
7. Applicable to nonlinear solid mechanics too (plasticity).
8. Examples here were in H^1, also can be extended to H(div) and H(curl).
9. Use VMS (LoD) for material interfaces and multiscale.
10. Adaptivity framework